BUILDING DETECTION IN SAR IMAGERY

BY

RYAN MATTHEW STEINBACH

THESIS

Submitted in partial fulfillment of the requirements
for the degree of Master of Science in Electrical and Computer Engineering
in the Graduate College of the
University of Illinois at Urbana-Champaign, 2015

Urbana, Illinois

Advisers:

Professor Erhan Kudeki
Peter D. Dragic, PhD
Mark W. Koch, PhD, Sandia National Laboratories
Mary M. Moya, PhD, Sandia National Laboratories

Abstract

Current techniques for building detection in Synthetic Aperture Radar (SAR) imagery can be computationally expensive and/or enforce stringent requirements for data acquisition. I present two techniques that are effective and efficient at determining an approximate building location. This approximate location can be used to extract a portion of the SAR image to then perform a more robust detection. The proposed techniques assume that for the desired image, bright lines and shadows (SAR artifact effects) are approximately labeled. These labels are enhanced and utilized to locate buildings, only if the related bright lines and shadows can be grouped. In order to find which of the bright lines and shadows are related, all of the bright lines are connected to all of the shadows. This allows the problem to be solved from a connected graph viewpoint, where the nodes are the bright lines and shadows and the arcs are the connections between bright lines and shadows. For the first technique (simple graph grouping), constraints based on angle of depression and the relationship between connected bright lines and shadows are applied to remove unrelated arcs. The second technique (weighted graph grouping) calculates weights for the connections and then performs a series of increasingly relaxed hard and soft thresholds. This thresholding results in groups of bright lines and shadows produced from various initial threshold levels. These different groups will be labeled and interpreted according to their initial thresholds. Once the related bright lines and shadows are grouped, their locations are combined to provide an

approximate building location. Experimental results demonstrate the outcome of the two techniques. The two techniques are compared and discussed.

Acknowledgments

I thank Professor Kudeki for supporting and allowing me the opportunity to work on a project which gave me the chance to explore areas of research that I am passionate about. I also thank Peter Dragic for co-advising my research so the partnership with Sandia and the University of Illinois could occur and this research could continue.

From Sandia National Labs (Sandia), I thank Steve Castillo and Kristina Czuchlewski for approving the partnership and for helping to work through the paperwork needed for this collaboration between Sandia and the University of Illinois. I appreciate Wallace Bow's help and support navigating issues at Sandia and his support of this work. I also thank Josh Michalenko for being a sounding board for ideas during the early stages of the project. The creation and labeling of the SAR data was done by Jeremey Goold, Mark Koch, and Mary Moya (from Sandia). This data was integral to the success of this research and opened the door for this technique to be successful.

Special thanks to Mary Moya for guidance, suggestions, and support during the development of these techniques, as well as comments and suggestions on the various drafts of this document.

And finally, special appreciations and thanks to Mark Koch for being an adviser and mentor throughout this whole project, for providing guidance and suggestions at all stages of the project, for being a sounding board and providing

discussion and criticism on various ideas for detection techniques, and for support on all other aspects of this project big and small.

This work was supported by PANTHER, a Laboratory Directed Research and Development (LDRD) Project at Sandia National Laboratories. For additional information about PANTHER, please contact Kristina Czuchlewski, PhD, krczuch@sandia.gov. Sandia National Laboratories is a multiprogram laboratory operated by Sandia Corporation, a Lockheed Martin Company, for the United States Department of Energy's National Nuclear Security Administration under Contract DE-AC04-94AL85000.

Portions of this thesis were previously published by the author. These portions are being reprinted here with permission from the International Society for Optics and Photonics (SPIE). The reprinted work was originally published under the title "Building detection in SAR imagery" and was written by R. Steinbach, M. W. Koch, M. M. Moya, and J. Goold. This paper was published as part of the 2015 SPIE Defense + Security Radar Sensor Technology XIX conference [24].

Contents

1. Introduction

With the vast amount of synthetic aperture radar (SAR) data available, processing the data manually can be difficult and very time-consuming. Algorithms from the areas of image processing and computer vision can help process the large amount of data collected using air-borne systems. Approaches in the areas of terrain classification, SAR artifact effects classification, and automatic target recognition allow an analyst to concentrate on high level tasks. If an analyst can focus on the higher level tasks, he/she will be able to find items of interest quicker and/or process more data. SAR artifact effects refer to man-made objects that produce very specific and reproducible effects when interacting with radar. Examples of these effects include bright lines and shadows. Bright lines are the result of the corner reflector created when the wall and ground meet. The shadow is the result of the scene behind the building being blocked by the building. Although these effects can be undesirable in some radar imagery applications, they are exploited in the presented techniques. This thesis proposes two techniques for building detection in SAR imagery that are efficient and effective in comparison to other proposed techniques. The building detection techniques presented make a few assumptions. First, an automated algorithm has already labeled the bright and shadow regions of a SAR image. Second, daily SAR images are gathered which have the same frequency, flight path, polarization, and depression angle. Third, there is a base knowledge of the size of buildings that are present in the images of interest. (This is needed since building sizes and shapes are so diverse and a starting point is needed for characterization.)

This thesis is organized as follows. Chapter 1 provides an introduction to the topic and presents the motivation and a high level overall approach. In chapter 2 related works are briefly discussed to provide the reader with justification and to further motivate the need for these new techniques. Chapter 3 presents an overview covering the assumptions made and explains what the results display. Discussions of the two techniques follow, covering common portions to both techniques (chapter 4), simple graph grouping (chapter 5), and weighted graph grouping (chapter 6). In chapter 7 the results of the two techniques are presented and compared to show their effectiveness. Finally, chapter 8 gives final thoughts, ties up loose ends, and presents possible future expansions. A brief overview of SAR is provided in the appendix for readers who are unfamiliar with SAR.

1.1 Motivation and Overall Approach

There is a need to classify, characterize, and detect the different regions of SAR images. Detecting objects such as buildings is very useful but poses several problems. Buildings have many unique shapes, sizes, and heights. This creates a complication because there are no fixed quantitative attributes that one can utilize to recognize a building. However, shadows and bright lines can be exploited to locate a building if they can be properly grouped. There are several techniques proposed by others which require multiple aspect images or a good interferometric SAR (InSAR) product. These techniques, however, can put demanding, stringent requirements on SAR data collection or are computationally expensive. An algorithmic approach is required to locate a building that is

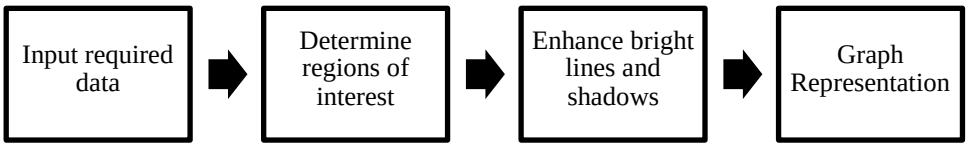

Figure 1.1: Block diagram for the portion of the technique common to the two proposed techniques.

efficient and not demanding on the gathering of SAR data and can handle images covering large areas (hundreds to thousands of square kilometers). Determining which bright lines and shadows are related without a priori information is a difficult task. Figure 1.1 is a block diagram outlining the common parts of the proposed techniques. The first block represents the required input data. Here, we assume access to a SAR image product with the shadow and bright lines classified. (Currently a technique based on superpixel segmentation [16] and classification using the Kolmogorov-Smirnov test [13], [22] and probabilistic fusion [19] is utilized by those providing the images. The superpixel segmentation creates groupings of pixels which are similar based pixel statistics. Kolmogorov-Smirnov test and probabilistic fusion are used to label the superpixels.) The second block finds subimages that contain possible buildings and focuses subsequent processing on the subimage regions. The third block enhances the shadows and edges by combing shadow fragments and determining the dihedral responses (this allows us to find the true bright lines). In the fourth block, we represent the problem as a large connected graph with nodes representing the shadows and bright lines, and with connections representing relationships between the shadows and bright lines.

Figure 1.2: Block diagram for the simple graph grouping.

At this point the two techniques start to differ. Simple graph grouping technique is a simple, deterministic technique which locates buildings by removing connections. In order to do this constraints are applied to reduce the number of connections and the building location is determined from the surviving subgraphs (Figure 1.2). These constraints are highly dependent on the style and size of the buildings as well as the expectations for building distributions. If these constraints are selected incorrectly, the results will be poor. Although this technique does require intelligent input based on best guessed a priori information, it will be shown that if the deterministic constraints are selected carefully, then the desired result of minimizing an analyst's low level task will be achieved.

It is desirable to improve simple graph grouping such that deterministic constraints are not required; instead, a more robust solution should be employed that provides flexibility in its approach for grouping connections into buildings rather than simply removing connections. In order to achieve this improvement, the bright line and shadow connections should be given weights. These weights indicate how well the bright line and shadow connections follow the assumptions made for the desired building's geometry. This improvement is the basis for weighted graph grouping.

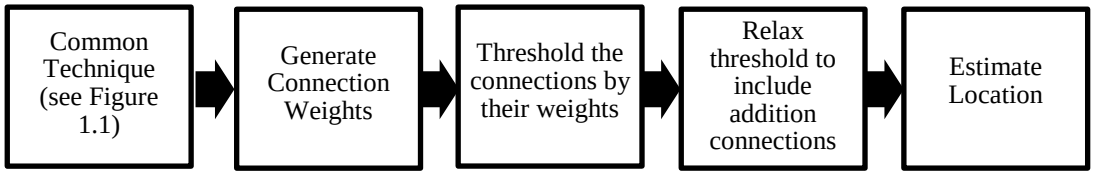

Figure 1.3: Block diagram for weighted graph grouping .

Weighted graph grouping generates the weights for the bright lines and shadows from the values that were used by the deterministic constraints in simple graph grouping. Instead of removing the connections outright, they are thresholded instead. This allows easy control over how strict or lax the requirements are for a connection to be considered valid. This could be achieved with simple graph grouping, but it would require many sets of intensive rules to produce similar results (and these rules would likely be highly dependent on a particular scene and it would not be simple to utilize the rules, as is, in another scene). Instead, with weighted graph grouping the threshold can be changed to achieve varying results, and if this technique was applied to a new scene, of significant difference, it would be simple to slightly change the weighting functions (much easier than writing new deterministic rules).

To create building estimates, the appropriate bright lines and shadow connections should be grouped. As previously stated, bright lines (produced by buildings) are created when the radar signal reflects from the intersection of a building wall and ground. The shadow, on the other hand, is the result of the building blocking the radar signal from scene. A bright line and shadow are connected if both of them are the result of the same building. A single building is

capable of producing multiple bright line and shadow connections, and all of these connections need to be grouped together. In order to group the connections, a thresholding technique is utilized. First, a strict threshold is applied to find connections that strongly agree with the building assumptions. If any such connection can be located, it is assumed that the shadow attached to this connection is produced by a building. The original strict threshold is then relaxed to search for additional connections attached to this shadow. The connections that fall within the strict or relaxed threshold are then grouped and are assumed to identify the bright lines and shadows which make up a building. From the bright lines and shadows in a group, a building location can be estimated (Figure 1.3).

1.2 Object Based Image Analysis

Object based image analysis (OBIA) is a very important tool for these techniques and provides the basis for how building locations are estimated. It is often very difficult to automate object detection using traditional image analysis (especially when SAR data is used). When an analyst does a task such as building detection, he or she will use context clues to pinpoint a building. These context clues include roads, driveways, fences, etc. However, when traditional image analysis techniques, only looking at the pixel level, are used, the benefits of contexts are eliminated. Utilizing OBIA, the power of human analysis plus the speed and power of a computer can be achieved. In depth discussion and examples of OBIA can be seen in the references authored by Jarlath O'Neil-Dunne [15], [17], [18].

OBIA exploits signal and image processing techniques to allow an algorithm to analyze an image similar to a human. The goal of OBIA is to create objects out of the pixels. These objects will then be used to analyze the image. For this technique, superpixel segmentation is an example of creating objects out of pixels. Once the objects are formed, the pixels contained by these objects can be used to characterize the objects, i.e. mean or variance. With the information, the objects can be labeled to imitate the context clues that a human analyst would utilize. Once analysis with the first set of objects is performed, pixel based analysis can be performed or new objects can be formed. This is similar to how a human analyst uses many different context clues and pixel values to understand an image.

Although the examples from O'Neil-Dunne's work show the power of OBIA using RGB (visible spectrum), IR (infrared), and LIDAR (Laser Illuminated Detection And Ranging) data, the perks of OBIA for SAR data are still obvious. In the techniques presented here, OBIA is not utilized so intensely as in O'Neil-Dunne's papers. However, similarly to the example OBIA techniques, the SAR imagery is segmented into superpixels and labeled. Using these data as well as the orientation of the segments and the pixel value statistics of the segments, a simple OBIA can be achieved to locate buildings. Discussions of different portions of OBIA and how they are used for building detection are presented in more depth in chapters 3 through 6.

2. Literature Review

Several techniques have been proposed for building detection, that detect the buildings by finding the building edges. In one technique [26], only bright lines were exploited to find buildings, whereas in another [7], [25], [28] shadows were added as another constraint. Bright lines result from the corner reflector created due to the interface between the building and ground [26]. To locate the buildings, SAR images with orthogonal flight paths were used to find multiple bright lines per building which produce parallelograms surrounding and outlining the buildings [25], [26] (Figure 2.1). To enhance the previous method, shadows were added to help with large building detection. The shadows help to provide another boundary that the bright lines do not provide [25]. While this technique worked very well, it requires careful flight planning to create orthogonal flight paths over the area of interest (which will not be available in all data sets). Building edges can also be detected using the watershed transform that is adjusted by bright lines and shadows [28]. The watershed algorithm finds boundaries by

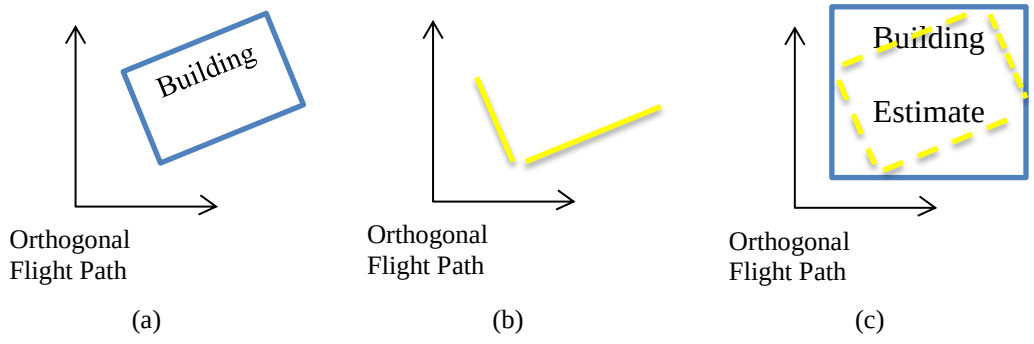

Figure 2.1: Simple example from [25], [26]. (a) Orthogonal flight path shown with an example building. (b) Bright lines for the building from the orthogonal flight path (yellow lines). (c) Parallelogram created from bright lines (yellow dashed lines) and the outlining bounding box for the parallelogram (blue rectangle). The blue rectangle is the building estimate. The example is exaggerated for ease of visualization.

filling regional minima until the two fills meet. At this point, the boundary is marked. Membership functions and rules were applied to objects, generated from detected bright lines and shadows, in order to create building hypotheses. The hypotheses were then used with the bright lines and shadows to find building edges [7].

Other techniques [2], [3], [6] did not utilize bright lines and shadows, but instead used Markov random fields (MRF) to generate labels which model the a priori information of the scene. The labels represent the actual values of the data being utilized and can be generated for multiple types of data: the amplitude and InSAR phase [3], the real and imaginary parts of multiple co-registered SAR images [2], and the height, calculated from the InSAR phase [6]. This technique generates a parameter for the MRF distribution which describes the label and depends only on the surrounding values. The larger this parameter, the higher the probability that the corresponding pixel is an edge.

All of the techniques presented above locate buildings by defining the buildings' edges. For example, the use of the Steger-operator to find the bright lines, orthorectification of the bright lines from the InSAR heights, and the iterative polygon hypothesize and test paradigm can be computationally time-consuming [25], [26]. The Steger-operator is a technique for line detection which utilizes an explicit model for a line. This technique allows for lines to be extracted with high accuracy [23]. Another approach uses extensive extraction, downselection, and combination of bright lines and shadows followed by the classification of features [7]. From these features, multiple hypotheses are

generated and tested to define building radar footprints. While robust, this technique can lead to a large number of hypotheses to search through. On the other hand, Markov random fields (MRF) for finding the edges generate a large number of values to compute the MRF edge parameter expectations [2], [3], [6]. This must be done across multiple iterations to ensure that the parameter converges and it is impractical for large images. These techniques have no region of interest operator and use computational resources on images that have no buildings or only a few buildings.

There are multiple other techniques presented in other papers. The techniques presented in these papers attempt to solve similar problems, but use very different tools and assumptions. These papers are briefly discussed in order to provide a complete picture of this problem. The topics help to give perspectives on the proposed techniques, as well as validate the assumptions.

Bright line and shadow features are used with a maximum likelihood inversion of a three-dimensional building model to perform building extraction [1]. Another technique uses only bright features and morphological operators to detect a building [4]. On the opposite side, buildings are found by exploiting the shadows [10]. Both features are exploited and buildings are located by utilizing a simple thresholding technique [27]. The techniques that use only bright features or shadows suffer because they do not utilize all the information. However, even when both types of features are used, simply thresholding the features is a naïve solution because it does not ensure that features are properly oriented and related.

3. Overview

In order to detect buildings, bright lines and shadows are utilized. Bright lines are a result of the corner reflector created where the building and the ground intersect, while shadows are the result of the SAR geometry. SAR creates shadows when an object in the scene reflects the RF energy and prevents the energy from reaching objects behind the reflecting object. Objects other than buildings can also generate bright lines and shadows. However, because we exploit generic assumptions about building sizes and knowledge about the system configuration, bright lines and shadows not created by buildings (i.e. power lines and metal fences for bright lines and cement and water for shadows) can be eliminated. Bright lines and shadows of interest can also be grouped together according to whether or not they are created by the same building.

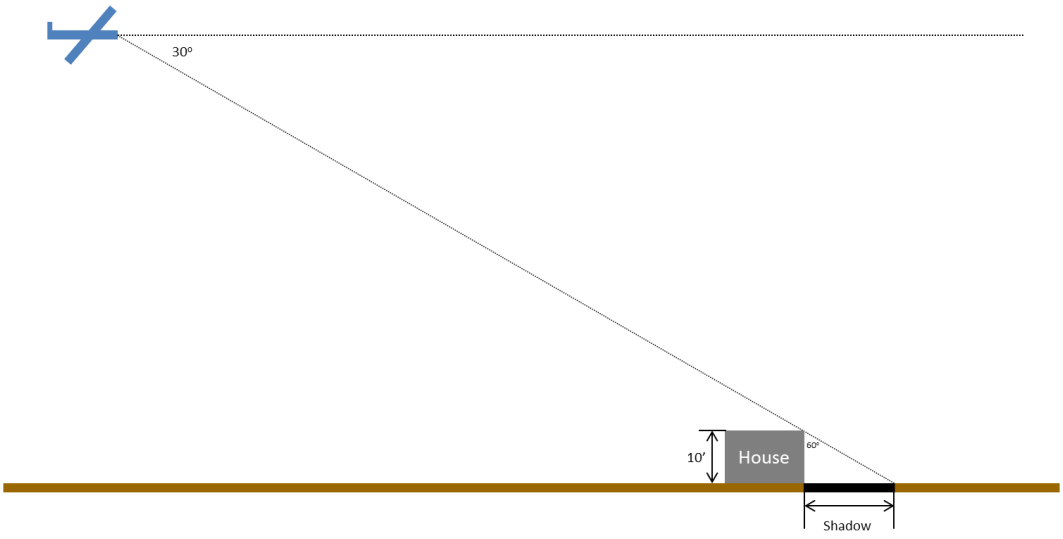

Figure 3.1: An example of how the angle of depression and building minimum height are used to determine the minimum length of a shadow.

A few constraints can be utilized to determine if the bright lines and shadows should be grouped. (Bright lines and shadows should be grouped only if they are created by the same building.) First, based on the angle of depression, a minimum shadow length can be determined (Figure 3.1). The taller an object, the longer its shadow. Buildings of interest can be assumed to have a minimum height. For the example above, it is assumed that the minimum building height is 10 feet and the angle of depression is 30 degrees. Therefore, the shadow must have a length of at least 17 feet.

Another constraint is that the bright lines and shadows must be in the same relationship. Bright lines will appear down range from shadows. Also, the distance and angle between a bright line and a shadow must be in an appropriate range to be part of the same building. If the distance is too great, then the bright line and shadow are not part of the same building; but neither can the distance be too small. If it is too small then the object is not long enough to be a building. Similarly, if the angle is too great, then the bright line and shadow will not be part of the same building. Figure 3.2 shows the acceptable region for the connected shadow's estimated center to be located in order for the arc connecting the shadow and bright line to be considered valid.

Once the bright lines and shadows are appropriately grouped (by building) they can be used to determine the location of a building. This is done by averaging the centroids of the bright lines and the centroids of the shadows. This provides an approximate location for the building, which should be

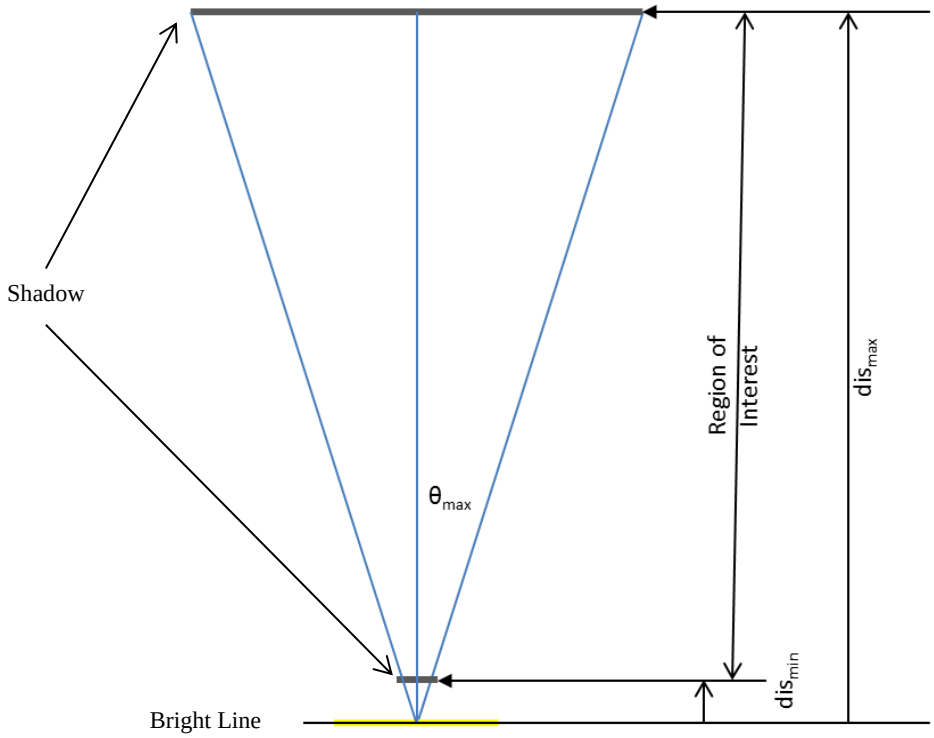

Figure 3.2: The acceptable range and angular region for the approximated center of a connected shadow under test.

contained somewhere within the bounding box of the building. However, the approximate location provides neither an accurate estimate of the building centroid nor a complete definition of the bounding box.

4. Common Technique

4.1 Data Preprocessing

A superpixel-based classification algorithm was applied to a number of SAR image products, some of which are formed from time-sequences of same-scene images. In a surveillance scenario, multipass images are created and can provide speckle-reduction and surface characterization properties not available in single images. The final class scores are determined using probabilistic fusion [19]. The output of the fusion is a test statistic and a p-value. Here the p-value represents the probability of getting that test statistic or higher. The p-values are used to generate the class labels (Figure 4.1) and indicate the likelihood that a

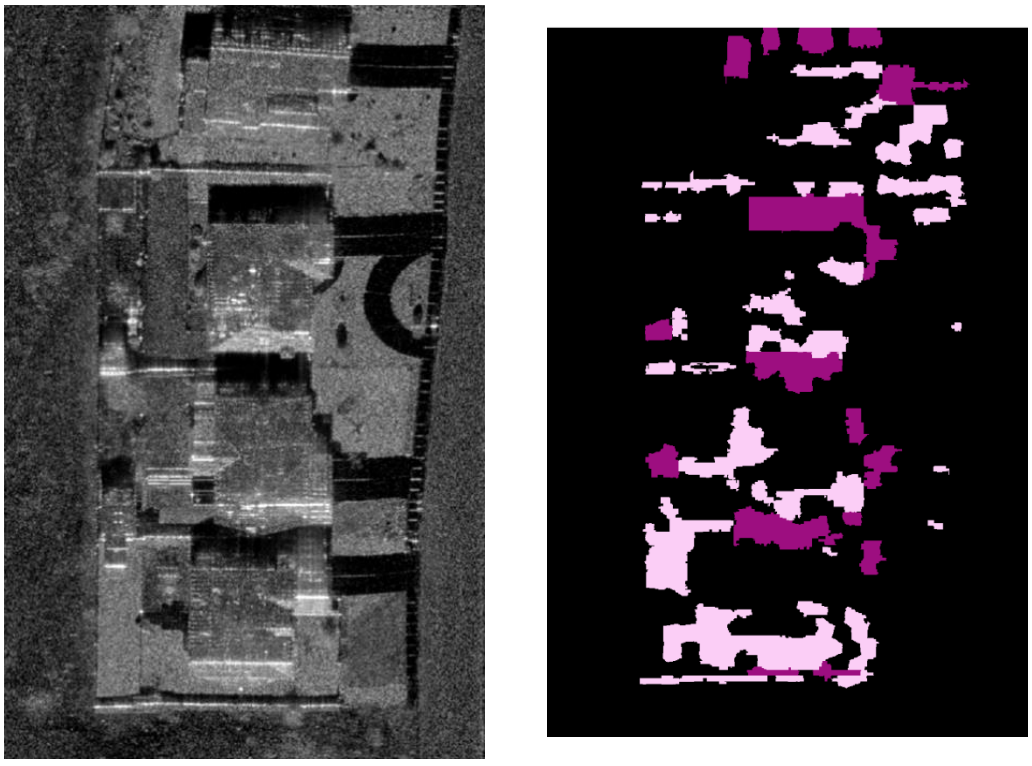

(a) (b)

Figure 4.1: Examples of the expected SAR products. (a) Median back-scatter image. (b) Bright lines (pink) and shadows labeled (magenta).

given pixel corresponds to a specific label [12]. The data preprocessing technique, presented in this section, was provided to give a more complete picture of the tools used to perform the building detection. This technique was created by researchers at Sandia National Laboratories. These researchers provided the raw SAR data and the labeled data produced by this technique.

4.2 Region of Interest

In order to utilize bright lines and shadows for locating the building, it is useful to first determine regions of interest where the bright lines and shadows could possibly correspond. To locate regions of interest an image of the scene is assumed to be available with bright line and shadow areas labeled. Figure 4.1 shows examples of the expected SAR products. The first step is to detect regions of interest (ROIs), which are subimages that could contain one or more buildings and allow future processing to be confined to these areas. First, the combination of bright line and shadow labels are dilated with no regard to class label. Then, the result of the dilation is grouped using four-pixel connection, and bounding boxes are found for these groups. Each of these bounding boxes is then checked to see if they contained both bright lines and shadow pixels. The idea behind this dilation and grouping is that a building will have bright lines and shadows relatively close to each other. If these bright lines and shadows, related to a building, are aggressively dilated they will overlap and create one blob. Figure 4.2 shows an example of the aggressive dilation. ROIs are extracted which surround one or more blobs containing both bright line and shadow.

(a) (b)

Figure 4.2: (a) Bright lines (pink) and shadows (magenta) before dilation. (b) Bright lines and shadow areas after dilation. They have morphed into blobs which can be used to locate the regions of interest.

4.3 Shadow Enhancement

Once the ROIs are located, the search for buildings is narrowed down to regions where the bright lines and shadows can be enhanced and located. To enhance the shadows, shadow-labeled pixels are conditionally dilated. The condition for dilation is p-values, which indicate the likelihood that a given pixel corresponds to a specific label. (P-values are discussed in section 4.1 and more in reference [12].) Conditional dilation is performed by first dilating the shadow labels. The newly included pixels are then checked against the p-values. If the pixel is greater than a threshold of β for the p-values, then it is kept as a valid labeled pixel. (P-values are a probability and are in the range of 0 to 1.) The idea is that pixels that are near to labeled pixels and have a large enough p-value, β or greater, are more likely to also be classified as that label. This step is important

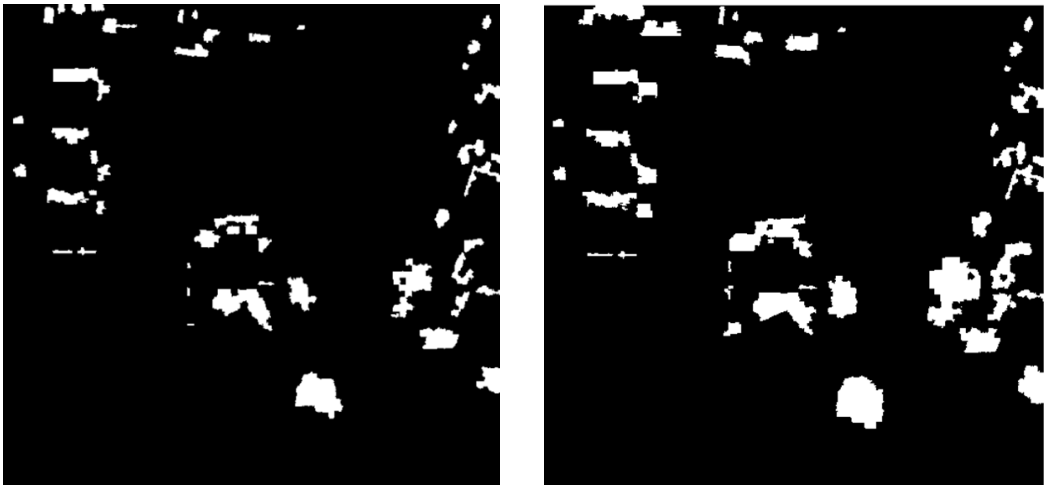

(a) (b)

Figure 4.3: The result of implementing the conditional dilation. (a) Pre-dilation, (b) post-dilation.

because it allows pixels that are truly part of a shadow but not labeled as shadow to be included in the shadow label. Figure 4.3 shows the difference between the pre-dilation shadow labels and the post-dilation shadow labels.

4.4 Bright Line Enhancement

In order to enhance the bright lines, the mean and variance statistics of the bright lines are estimated. This is required because the bright line labels contain more pixels than just the bright lines. The statistics are computed in the quarter power domain so the distribution will be approximately Gaussian. Then the assumption can be made that all pixels greater than the mean plus two standard deviations are bright lines. Once these are obtained, the lines can be further located and enhanced using the power ratio test presented in [14]. The ratio test looks at the ratio of the mean of the values in the target region, the center white region, and the mean of the values in the clutter region, the outside white ring, see Figure 4.4c. The bright lines found from the bright label statistics can be seen in

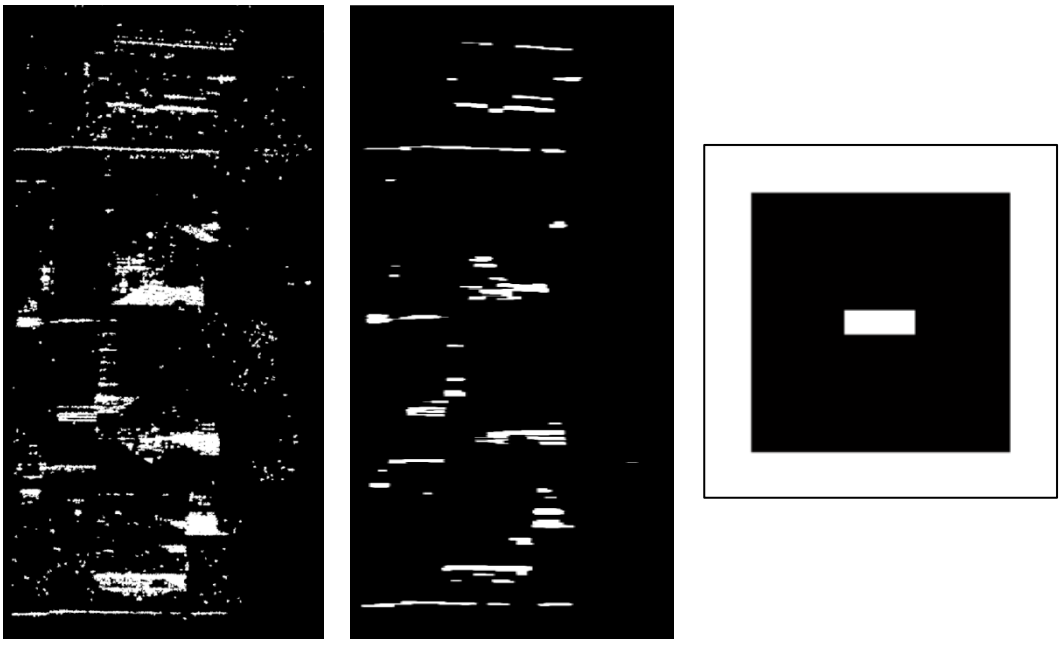

(a) (b) (c)

Figure 4.4: (a) The result of utilizing the bright statistic, in the quarter power domain, to find possible bright line pixels. (b) The result of enhancing the bright lines. (c) The regions used for calculating the ratio to determine whether the pixel is part of a line or not. The outside white ring is the clutter region, the black region is the guard region, and the center white portion is the target region.

Figure 4.4a, and the result of the power ratio test can be seen in Figure 4.4b. An example of the power ratio test regions can be seen in Figure 4.4c. If the ratio is above some threshold, the pixel is set as a bright line pixel. To ensure that the bright line pixels are connected appropriately, three sets of increasing line dilations and erosions are performed.

4.5 Graph Representation

The bright lines and shadows can be grouped to find a building because both bright lines and shadows are the result of the radar interacting with a building. Bright lines are the result of the corner reflector created when the wall and ground meet. This also locates the side of the building that is parallel to the

flight and closest to the receiver. The shadow is the result of the scene behind the building being blocked by the building. Just as with the bright lines, the shadows indicate the side of the building parallel to the flight path; however, it is the side farthest from the receiver. Although these effects may seem undesirable, for this purpose they are beneficial. (Bright lines and shadows are referred to above as SAR artifact effects.) A graph representation is used to group the bright lines and shadows into a building. Each shadow and bright line is assigned to a node in the graph. The arcs of the graph indicate the relationship between the nodes. The connection is based on the centroid of the bright lines and the shadows. The graph is fully connected in that all of the bright lines are connected to all of the shadows by their centroids. There is no need to connect all of the bright line centroids to other bright line centroids and all of the shadow centroids to other shadow centroids because these will be appropriately grouped by finding the connections of bright lines and shadows. (That is, if there is more than one bright line or shadow label for a given building, they will be appropriately grouped to the same building simply by connecting the bright lines and shadows.)

5. Simple Graph Grouping

Once all of the connections are made between bright lines and shadows there are no clear groups for buildings. The connections must be narrowed down in order to locate buildings. Some simple constraints are utilized to narrow down the connections.

5.1 Graph Reduction using Constraints

First, the length of the shadow is verified. If the shadow is too short then it cannot be the result of a building. The minimum length of a shadow can be calculated from the angle of depression and the minimum allowable height of a building (Figure 3.1). Any shadow that is shorter than the minimum, as well as any connections to this shadow, is discarded. As stated previously, bright lines should be closer to the receiver than their connected shadow. Thus, any connections between bright lines and shadows where shadows are closer to the receiver are also discarded. Another constraint limits the angle between the range direction and the bright-shadow connection vector. This further reduces connections between bright lines and shadows, since the angle must also not be too large (Figure 3.2).

Once all of the bright lines and shadows in a group are known, the building location can be approximated. First, the shadow centroids and the bright line centroids are separately averaged. Then these two averages are averaged. What this ensures is that if there are a greater number of bright lines or shadows, the result will not be skewed one way or the other. With this result the building is now located. It is important to note that this is not a bounding box of the building

or the exact center of the building. This also is very useful for narrowing down the location of the building so a more robust or computationally expensive technique can be utilized.

6. Weighted Graph Grouping

Just like at the start of Simple Graph Grouping, there are connections between all of the bright lines and shadows. Again the number of connections must be narrowed down in order to locate the valid buildings. However, instead of utilizing simple deterministic constraints that remove connections that break a single rule, the connections are weighted. With the connections weighted, a variety of different techniques can be utilized to find the combination of valid connections. With these combinations, an approximate location of the buildings can be found.

In order to produce a weight for a connection, a function must be created to convert characteristics of the connection to a weight. Similarly to Simple Graph Grouping, the length and angle of the connection are utilized. The weighting functions makes assumptions similar to those of Simple Graph Grouping, but the assumptions will not be deterministic in nature. The combined weights with values closer to zero are more likely to be a valid connection between a bright line and shadow. To find the connections which make up a building, a technique similar in nature to conditional dilation will be exploited. The technique makes use of strict thresholds. It is necessary to use strict thresholds to find valid buildings because the number of buildings in a given region of interest is unknown. If a shadow has a connection after a strict threshold, meaning it has a strong weight (low values), then connections to that shadow with weaker weights (high values) will also be included as valid connections to that shadow.

6.1 Edge Weighting

In order to produce the weights for the connections, the angle and distance values associated with a given connection need to be mapped, converted, and combined. This weighting technique can be completed by training from a known data set with labeled building; however, because this is a proof of concept experiment and the available data set is limited and unlabeled, a logistic function is used to obtain a weight for the distance or angle value. The logistic function (Figure 6.1) was selected since it rescales input values to a value ranging from zero to one. The disadvantage of the logistic function is that it quickly reaches its asymptotes of zero and one. This is a problem since we are looking at angles in the range of -180 to 180 degrees and distance values zero to orders of

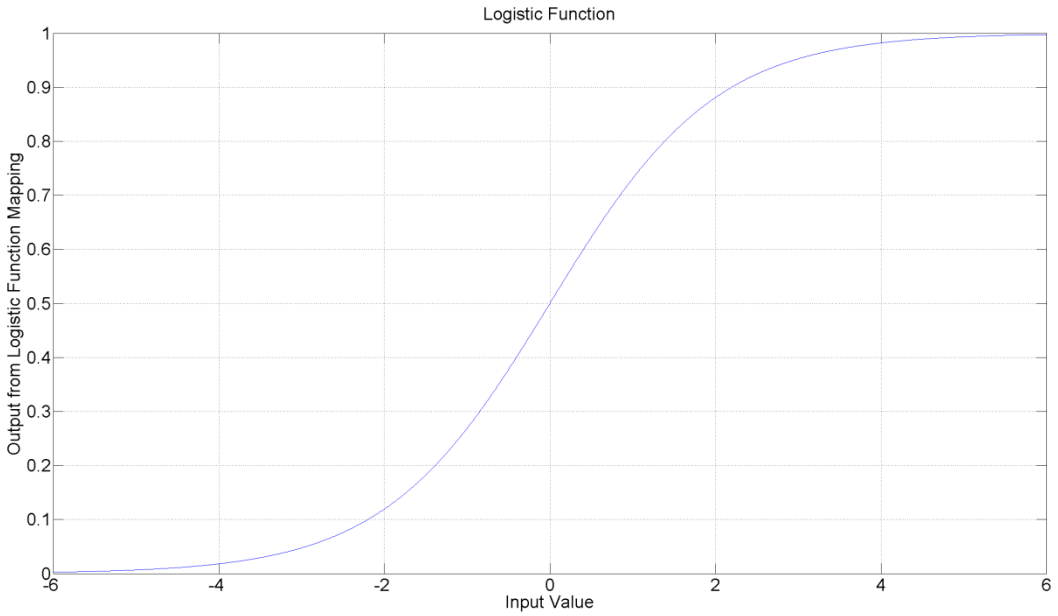

Figure 6.1: The logistic function is used to map input values to output values in the range of zero to one. It is obvious that the logistic function converges quickly to zero, at approximately -6, and to one, at approximately 6. With this observation it is clear that the angle and distance values must be rescaled from the original values to values that can be used with the logistic function.

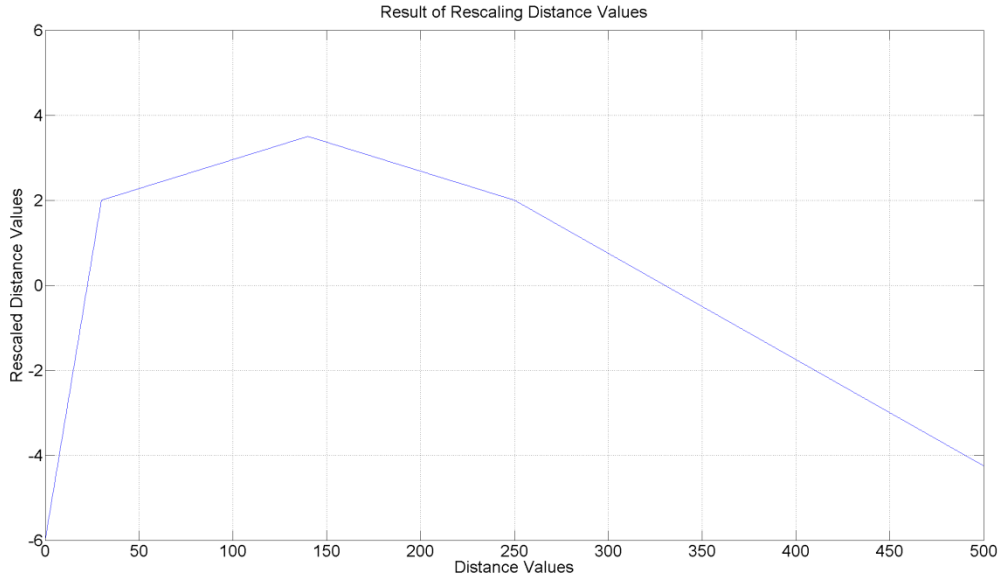

(a)

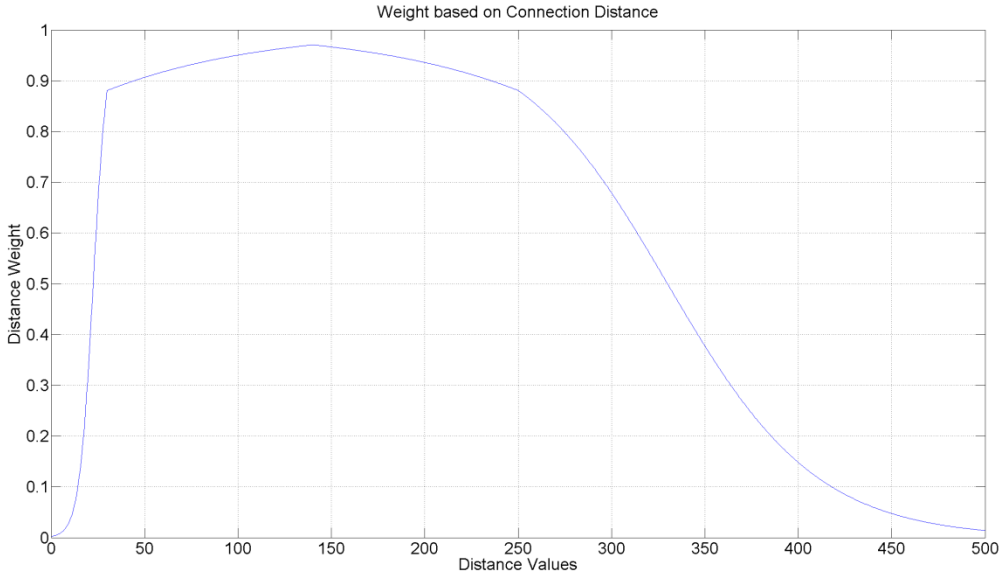

(b)

Figure 6.2: This figure shows the rescaling and weighting function for the distance values. (a) This is the distance rescaling function from the distance values to the values that will be used with the logistic function. The shape of the mapping is based on the assumptions about the buildings that are being searched for. The mapping gives preference to connections that fall in the range of η to τ (these values are mapped to values greater than zero producing weight greater than 0.5). (b) Plot of the distance weighting function. All of the values are in the range of 0 to 1.

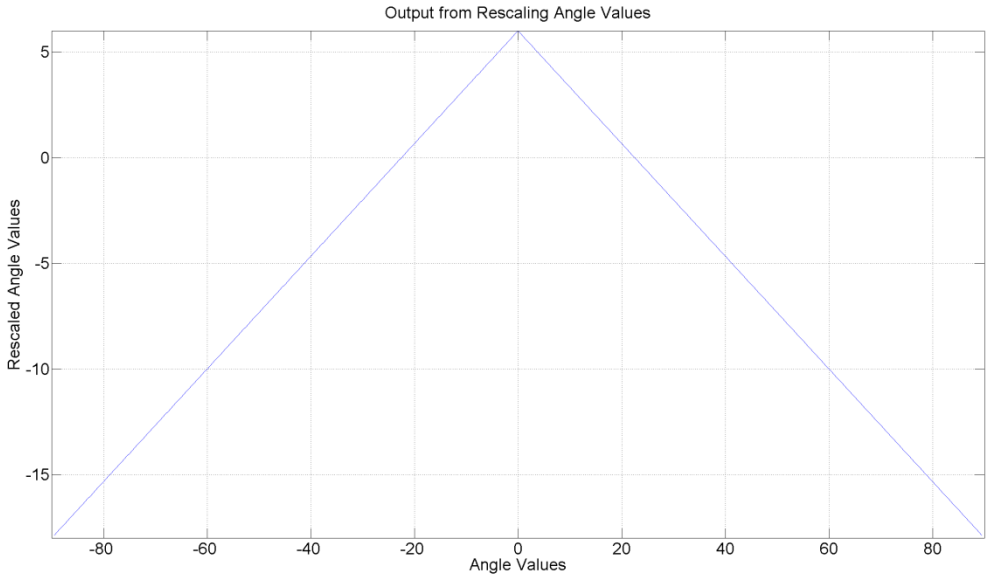

(a)

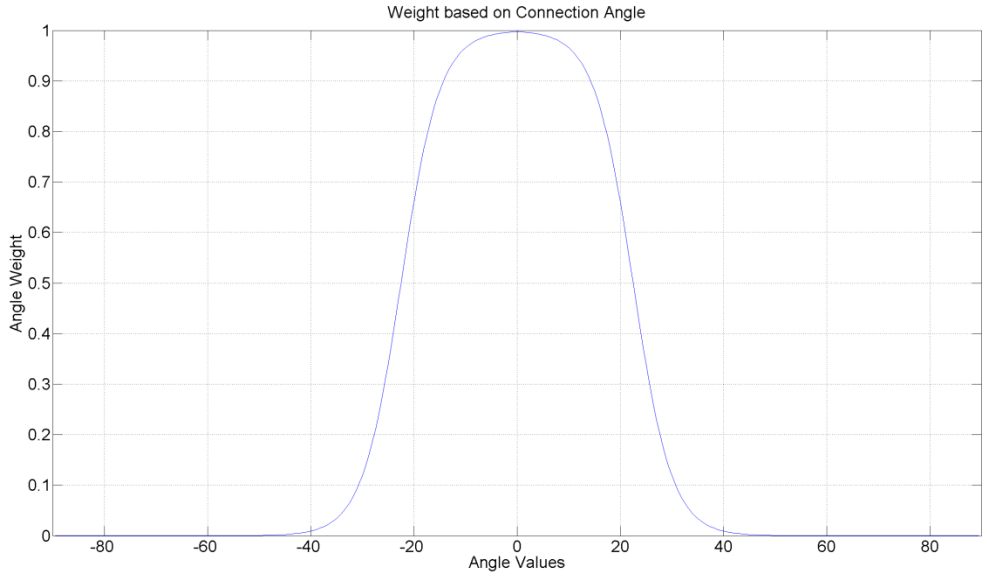

(b)

Figure 6.3: This figure shows the rescaling and weighting function for the angle values. They were created similarly to the distance case presented in Figure 6.2. (a) Plot of the angle rescaling. This mapping is symmetric about zero degrees. The mapping results in a preference of angle values in the range of $\pm\theta$. (b) Plot of the angle weighting function for the angles. All of the values are in the range of 0 to 1. Unlike the distance case where no value is approximately one, an angle value of zero degrees is the ideal result for a connection and therefore receives a weight approximately equal to one.

magnitude greater than one. In order to solve this problem the values are first mapped to an appropriate range that can be used by the logistic function (Figure 6.2a and Figure 6.3a). These mappings were created using the assumption presented in chapter 3. The mappings are similar in nature to the deterministic constraints. The mapped values are then passed to the logistic function to convert the values to the range of zero to one. For each individual case, angle and distance, values closer to one are more likely to be a valid value for that case (Figure 6.2b and Figure 6.3b).

Once the weights for the individual cases are found, they need to be combined so grouping of the connections can be performed. This combined weight could also be looked at as a pseudodistance metric if one wished to use another technique, i.e. k-nearest neighbors. To ensure flexibility in the use of the weights, values closer to zero are more likely to be valid connections. (This is the reverse of the individual case.) This switch in what value of the weight indicates a valid connection is due to the equation used to combine the individual weights for distance and angle. The combined weight is produced by using a weighted sum and subtracting this value from the maximum (Figure 6.4). Currently, the angle is slightly favored over the distance because there is a much wider range for the distance of an edge between a bright line and a shadow; buildings are unique in size, but the angle of the edge connecting a bright line and shadow should be close to zero degrees if it is a valid connection. (This is discussed in chapter 3.) Equation 6.1 shows how the individual weights are combined.

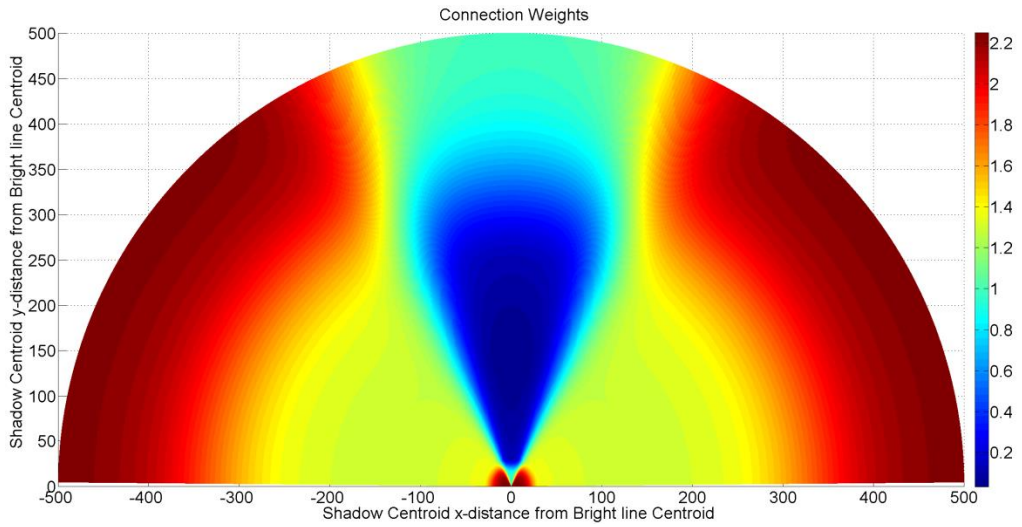

Figure 6.4: The result of using equation 6.1 to combine the individual distance and angle weights. The lower weights (blue) are a similar shape to that of the discrete case. The larger weights (red) are connections that are not likely to be the result of a building. This follows the assumptions presented in chapter 3. The bottom center of the plot represents the centroid of the bright line. Every other point represents possible shadow centroids and the combined weight for the connection that connects that shadow and bright line centroid.

$$\text{Combined Weight} = 2.25 - (1.25 \cdot \text{Angle Weight} + \text{Distance Weight}) \tag{6.1}$$

In the next section, the results of combining the weights are presented. If the low values (blue) of the combined weights, Figure 6.4, are compared to the accepted discrete case (Figure 3.2) the blue region has a similar shape to the triangular constraint region.

6.2 Combining Edges to Find Buildings

Once the weights are determined for the connections, the connections can start to be grouped. This can be looked at as clustering as well, but for this technique no clustering technique is utilized. Instead, a set of increasing thresholds is applied to find which bright lines and shadows are related. To do this a strict threshold is first applied to all of the weights. If, after the first

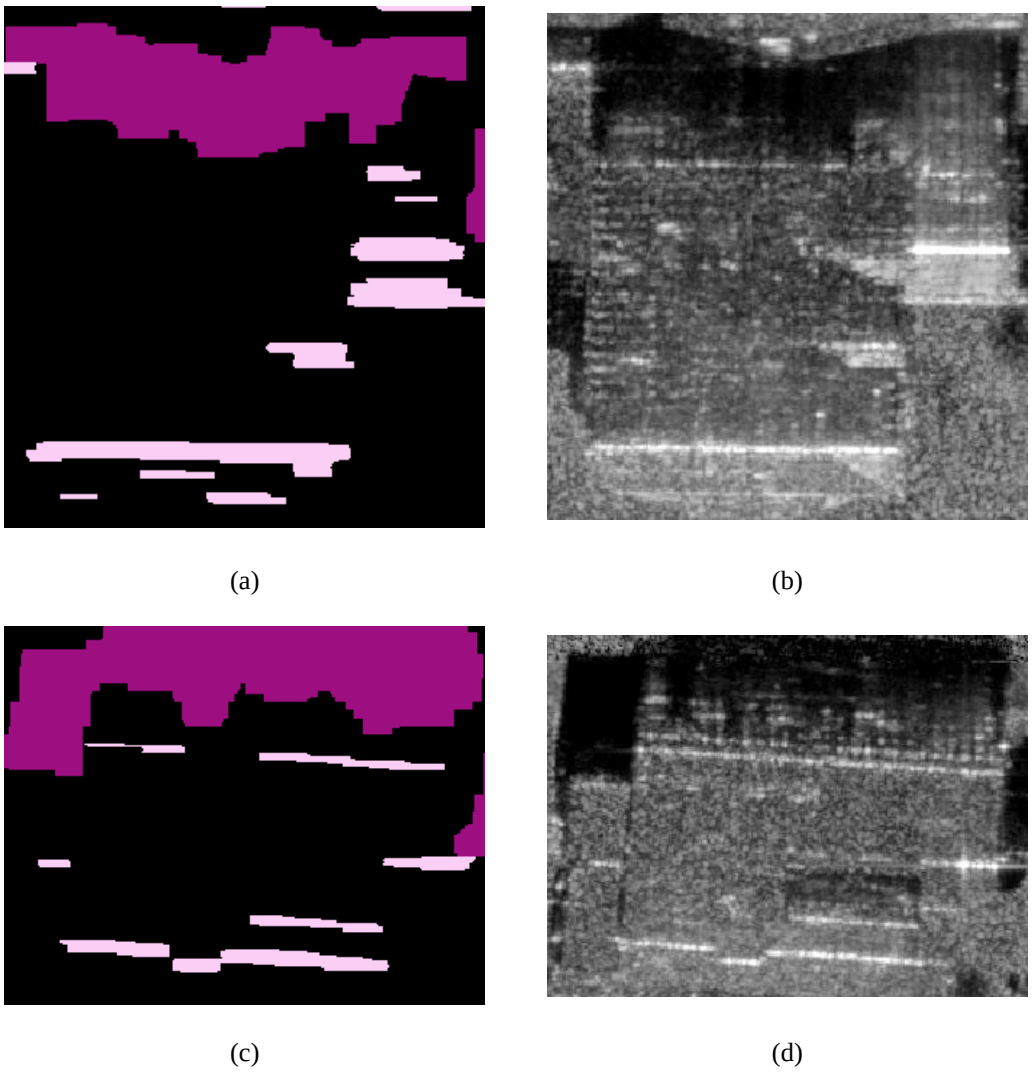

(a) (b)

(c) (d)

Figure 6.5: Examples of buildings which could have multiple connections with different weights. (a) Bright line and shadow labels for an L-shaped building. (b) SAR image of an L-shaped building. (c) Bright line and shadow labels for a building were the bright line is broken into multiple pieces. (d) SAR image of a building were a bright line is broken into multiple pieces.

thresholding, there are any valid connections, then the threshold is relaxed. If there are any further connections that fall within the relaxed threshold *and* are connected to a shadow which already has a valid connection (accepted under the strict threshold), then that connection will also be accepted as a valid connection. This is a safe technique to employ because if a shadow has a valid connection to a bright line it is likely that that shadow is the result of a building. Since the data

that is being utilized is from SAR imagery there is a chance that the bright lines may be separated into separate portions. This could result in multiple connections to the same shadow resulting from a single bright line broken into multiple pieces when they are labeled: however, depending on the layout of the difference portions of the line, this technique could produce varying weights (see Figure 6.5 c & d). This issue could also arise if the building is not a traditional shape, i.e. L-shaped (see Figure 6.5 a & b).

However, using this technique poses a problem because a hard threshold is required in order to group the connections and find buildings. This is due to the fact that the number of buildings in a region of interest is unknown. (On the other hand, if the number of buildings were known then this technique could utilize traditional clustering algorithms to cluster the connections into the appropriate number of buildings.) The selection of the threshold will directly affect the quality of the result achieved and is similar in nature to a Neyman-Pearson threshold selection. The Neyman-Pearson technique attempts to maximize the probability of detection while ensuring that the probability of false alarm remains less than or equal to a predetermined value [11]. For this problem, a false alarm would be a decision that there is a building when none is present. However, this must be weighed against missing a building detection. To deal with this issue, three sets of "strict" thresholds will be used: buildings detected under the strictest threshold are very likely to be buildings, buildings detected under the second strictest threshold are moderately likely to be buildings, and buildings detected

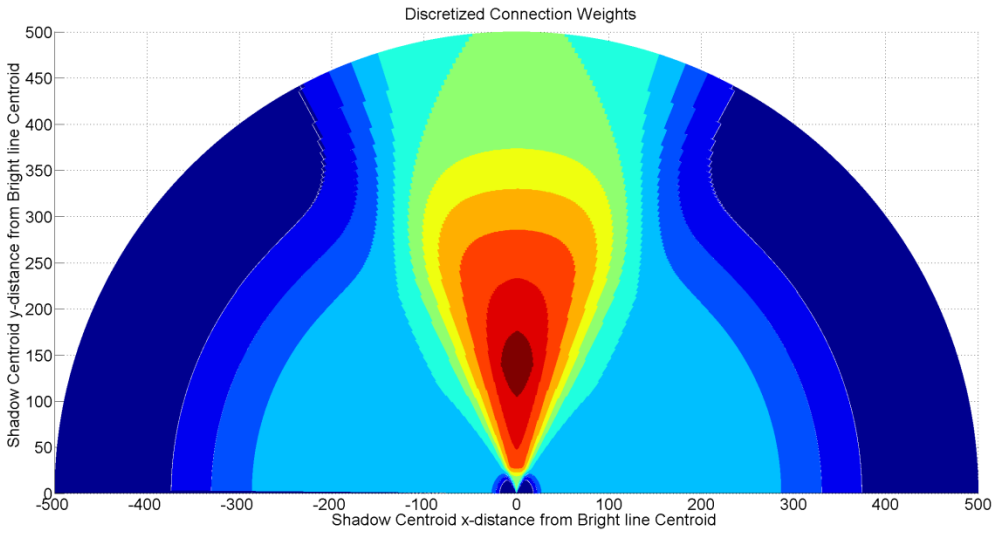

(a)

<0.05	<0.1	<0.25	<0.5	<0.75	<1.0	<1.25	<1.5	<1.75	<2.0	≥2.0

(b)

Figure 6.6: (a) Discretized version of the weight plot. Just as in Figure 6.4, the bottom center of the plot represents the centroid of the bright line. Every other point represents possible shadow centroids and the combined weight for the connection that connects that shadow and bright line centroid. (b) This is the color map showing the values of the thresholds used to discretize the weights.

under the third threshold are less likely to be buildings. The justification for assuming this is just like a Neyman-Pearson detection problem. The stricter the threshold, the less likely the detection is a false alarm, but it is more likely that there will be missed detections. On the other hand, if a weaker threshold is used, it is more likely for there to be a false alarm but it is less likely that there will be a missed detection. If the weights from Figure 6.4 are discretized to groups of increasingly relaxed thresholds (larger thresholds), as shown in Figure 6.6, the decision to use the three threshold techniques is clear. The groups that are produced by the larger thresholds will be accepted as valid connections. This will minimize missing buildings, but it will result in accepted invalid connections and subsequent false labeling of buildings.

Although weighted graph grouping appears more complex than Simple Graph Grouping, there is little increase in computational complexity. The weighting is calculated by using two maps, one being the logistic function, and the weighted summing equation (equation 6.1). To group the connections in Weighted Graph Grouping, the weights are thresholded. This is similar in complexity to the simple deterministic rules used in Simple Graph Grouping.

7. Results

This chapter contains the result of applying the two building detector techniques to a scene with all of the required product types and labels. The results presented here are for a single region of interest generated from the common technique. Figure 7.1a shows an extracted region of interested (presented in section 4.2) which contains enhanced bright lines and shadows (presented in section 4.3 and 4.4). These are examples of results using the common portions of simple graph grouping and Weighted Graph Grouping. As previously stated, it is important to enhance the bright lines and shadows to achieve a better result.

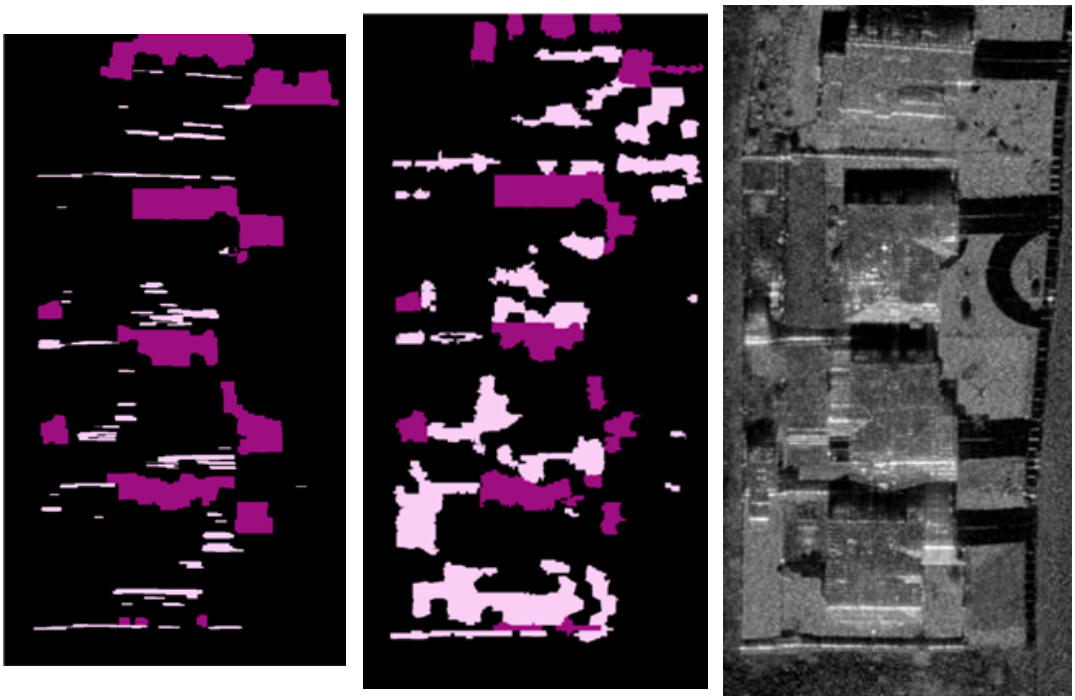

(a) (b) (c)

Figure 7.1: Region of interest extracted from an image. The result of the technique explained in section 4.2 (a) Enhanced bright line and shadow labels. This is the result for the techniques presented in section 4.3 and 4.4. The magenta patches are shadows and the pink patches are bright lines. (b) Original labeling of bright lines and shadows. (The colors are the same for Figure 7.1a.) (c) SAR image for the ROI being presented in the results.

When Figure 7.1a is compared to the original data labeling, seen in Figure 7.1b, it is clear that the bright lines and shadows have been more accurately labeled. This can be observed by looking at the SAR image (Figure 7.1c).

Figure 7.2a shows all of the bright line centers connected to all of the shadow centers. This is the base graph representation for this region of interest. The graph representation is the final part of the common technique and is presented in section 4.5. This image makes it clear that there is a complicated combination of bright lines and shadows. With the current number of connections it is extremely difficult to visually detect a building. Thus, it is important to reduce the number of connections in order to detect a building. The technique for the reduction of connections is where simple graph grouping and weighted graph grouping differ. Section 7.1 presents and discusses the results of reducing connections and locating buildings by Simple Graph Grouping, and section 7.2 presents and discusses the results for Weighted Graph Grouping.

7.1 Results of Simple Graph Grouping

Simple graph grouping is described in chapter 5. The results presented in this chapter are a continuation of the results shown previously. Since this test is based on strict deterministic rules, the quality of the results is strongly dependent on the rules selected when the technique is executed. Therefore, it is important when interpreting these results to remember that their quality is based on the a priori knowledge of the style and size of the building in the test scenes.

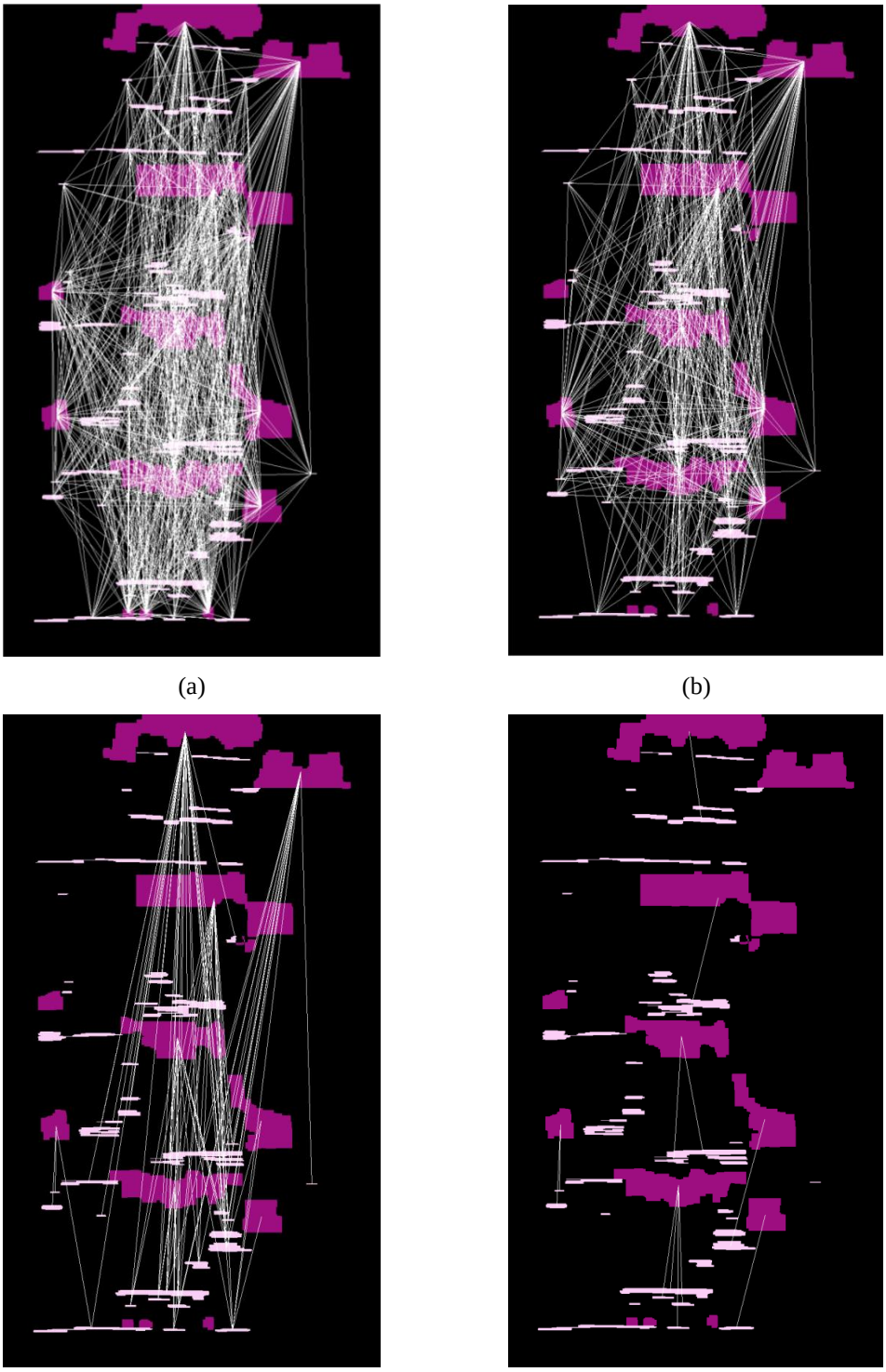

(a) (b)

(c) (d)

Figure 7.2: (a) All of the bright lines connected to all of the shadows. No connections removed. (b) Connections removed from failing the angle of depression requirement. (c) Connections removed from failing the angle requirements. (d) Connections removed from failing the distance requirements. There are two false detections in this region of interest, which result from the limitations of the classifier and the conditional dilation. The driveways were considered as shadows which confused the detector.

These results show that with properly selected rules one can achieve the desired results. Although this technique does not automatically generate the rules for the algorithm, it still addresses the problem presented in chapter 1. This technique will still require an intelligent analyst to provide rules based on his or her knowledge of the scenes under observation; however, it will save the analyst time by automatically locating possible buildings over a large amount of imagery and area. Although it could be considered a disadvantage to have to select rules or input parameters, this also allows the algorithm to be simpler to understand for the analyst than other black box machine learning algorithms, i.e. neural networks. It is important that an analyst be able to understand the algorithm so he or she can easily utilize it and understand the outputs.

Simple graph grouping reduces the connections by applying three constraints. The constraints are presented as if they were performed in a particular order, but in reality they are applied simultaneously. These constraints are introduced in chapter 3 and are depicted in Figures 3.1 and 3.2. The angle of depression reduction test (see Figure 7.2b) does not greatly reduce the connections, but it does remove connections that will increase the quality of the results. The constraint that reduces the most connections is the angle of the connecting vector. This constraint eliminates two connections issues. First, it ensures that bright lines are not connected to shadows that are closer to the receiver. Second, it removes connections that are at too broad an angle for the bright lines and shadows to be related. Figure 7.2c shows the results of this

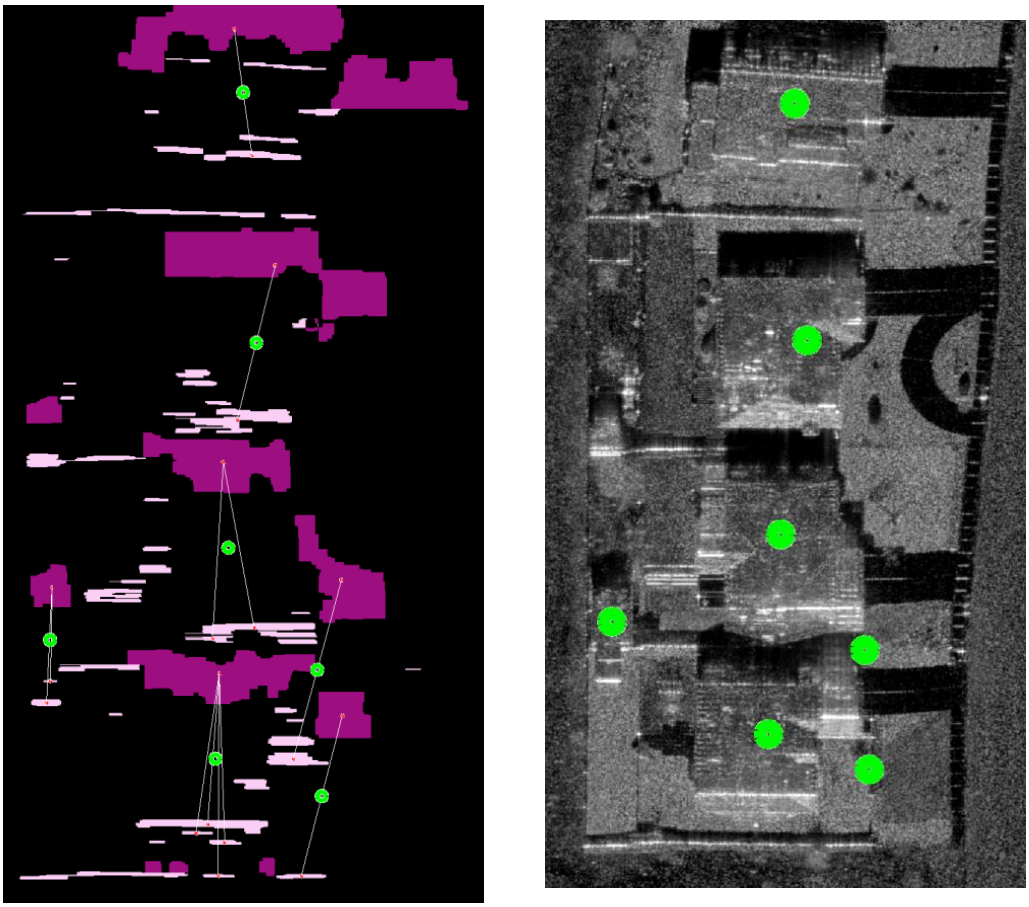

(a) (b)

Figure 7.3: Building location estimates. (a) The estimates are obtained by averaging the bright line centers and averaging the shadow centers. Then these averages are averaged. (b) Estimate shown on the SAR image.

constraint. The last constraint applied is the distance constraint, which checks that the shadows are not too close to the bright lines or that the shadows are not too far from the bright lines. If either of these occurs, then the shadow and bright line are not part of the same building. The result of this constraint can be seen in Figure 7.2d. Once the groups are determined, the building location estimate can be obtained. This is done by first averaging the centers of the bright lines and averaging the centers of the shadows. Then the two averages are averaged. Figure 7.3 shows the results of determining the estimates.

7.2 Results of Weighted Graph Grouping

Weighted graph grouping is described in chapter 6. The results presented in this chapter are a continuation of the results shown previously at the beginning of chapter 7. Just as with Simple Graph Grouping, the results of weighted graph grouping are dependent on the quality of the mapping and combination functions utilized. Therefore, it is important when interpreting these results to remember that the quality of the results presented was achieved based on the a priori knowledge of the style and size of the building in the test scenes. This technique, unlike Simple Graph Grouping, is more sophisticated and could allow the possibility of teaching the weights for use for the connections. If there is not a training set available, this technique could require an intelligent analyst to provide adjustments to the mapping, logistic, or combination equations.

Unlike Simple Graph Grouping, weighted graph grouping does not remove connections; it instead groups the connections. However, weighted graph grouping does not require that all of the connections be utilized, nor does it assume a certain number of buildings. The grouping is achieved by using a strict threshold on the connection weights followed by relaxing that threshold to include additional connections with larger weights (for the combined weights, the larger the value, the worse the connection). To generate the weights, the length and angle values of the connection are first individually calculated and then combined. Further information on the calculation and combination of the individual weights is presented in chapter 6. The thresholding and relaxing of the threshold are discussed in section 6.2. As discussed in that section, the thresholding and

relaxing of the threshold were performed three times with increasingly relaxed thresholds. This was done to minimize the number of false alarm buildings while still finding the buildings that do not fit the assumed building model well. However, when these multiple thresholds are used, the confidence in the building estimates is in a range depending on the threshold utilized. Depending on the threshold used, the estimate will be labeled strong, moderate, or weak.

Just as with the selection of the parameters for the constraints, used in Simple Graph Grouping, the selection of the three thresholds and how to interpret the different building estimate labels requires care. Although having three different building estimate labels can complicate detection, the benefits, discussed below, allow the exclusion of false detection or the inclusion of possibly missed. Similarly to Simple Graph Grouping, once the groups are determined, the building location estimate can be obtained. (These estimates will be labeled as strong, moderate, or weak according to the threshold which the connections were grouped under.) The building estimate is found by first averaging the centers of the bright lines and averaging the centers of the shadows. Then the two averages are averaged.

Figure 7.4 shows the results of determining the strong estimates. To show how weighted graph grouping is able to produce groupings of connections, Figure 7.4a shows all of the connections created using the common techniques discussed in chapter 4. The results of the first strict threshold application are presented in Figure 7.4b. It is obvious from the connections that they fall under the desired region (see Figure 6.6). The results from relaxing the first threshold and

accepting additional connections are shown in Figure 7.4c. When Figure 7.4 b & c are compared it is clear that additional connections are accepted. The building estimates with a strong label are also shown in Figure 7.4c. These results are overlaid on the SAR image, seen in Figure 7.4d. The results from the second, moderate threshold are presented in Figure 7.5 and are organized the same as the strong threshold results. Similarly, the weak threshold results are presented in Figure 7.6 and organized as before.

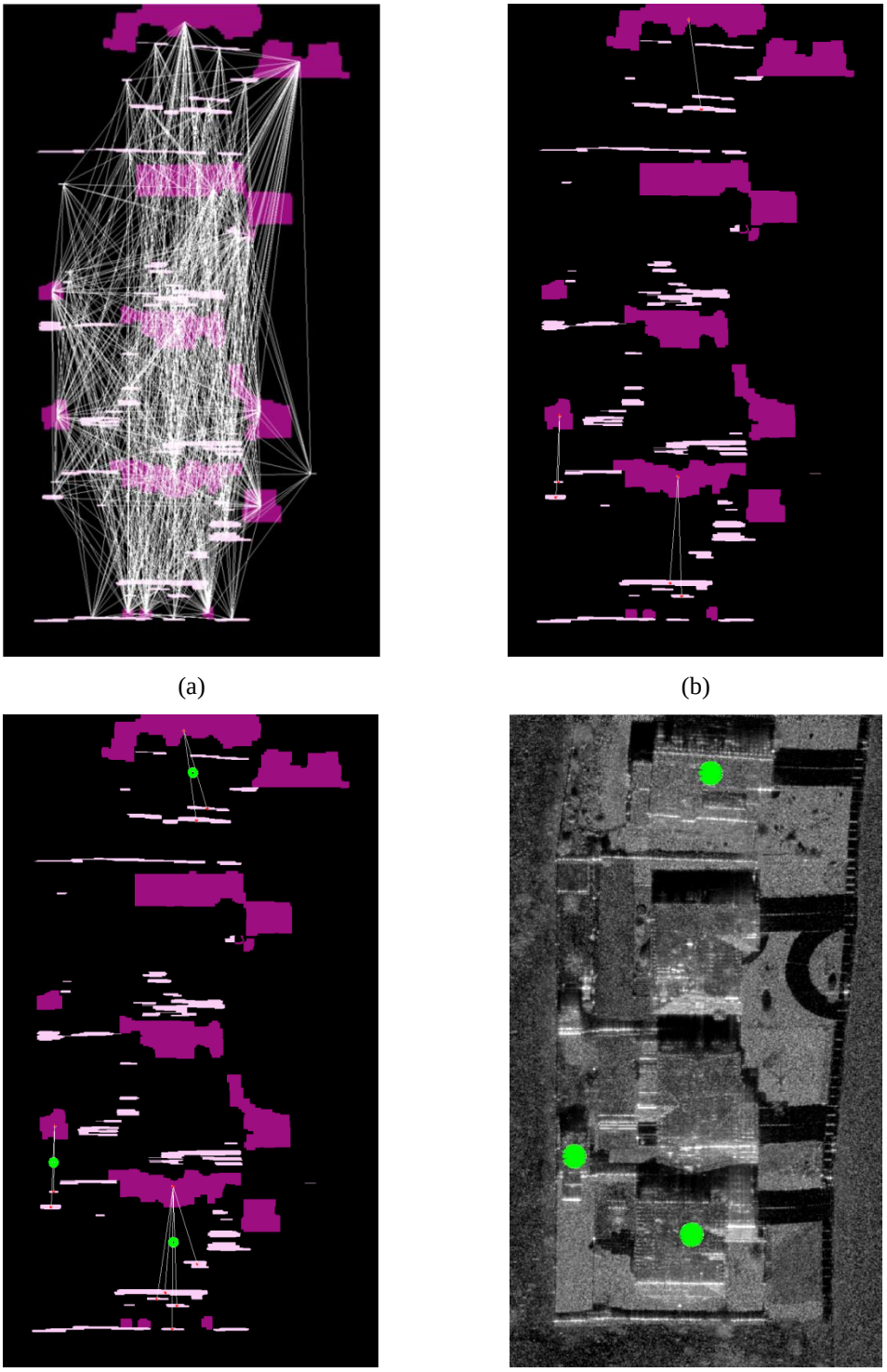

(a) (b)

(c) (d)

Figure 7.4: Strong threshold. Bright line labels are shown in pink and shadow labels are shown in purple. (a) All of the bright lines connected to all of the shadows. No connections removed. (b) Connections removed that are not below the low threshold. (c) Connections added if they are below the relaxed threshold *and* they are connected to a shadow that already has a valid connection under the strict threshold. Building estimates are shown in green. These estimates are given a label of strong. (d) Estimates are shown on the SAR image.

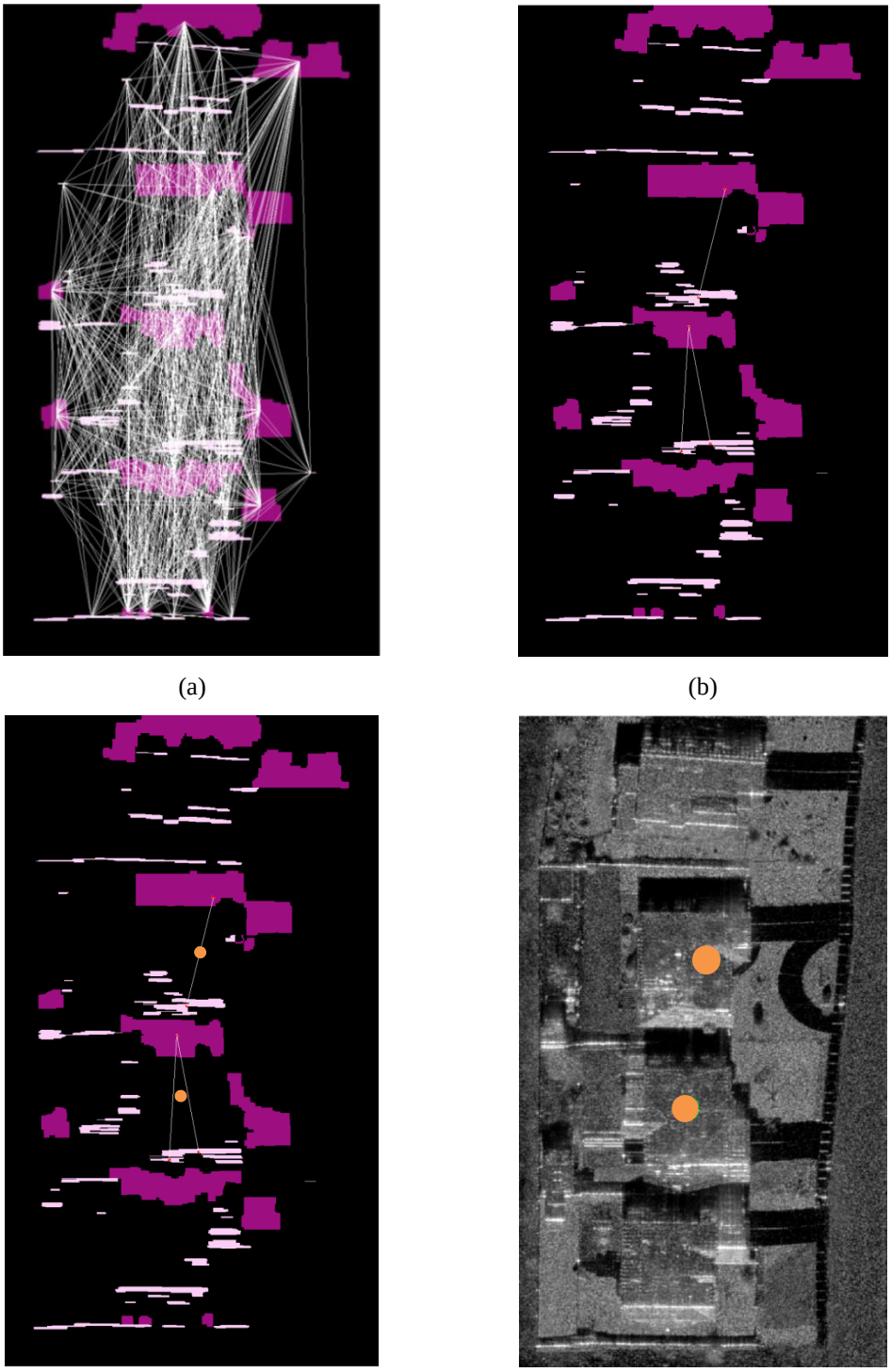

(a) (b)

(c) (d)

Figure 7.5: Moderate threshold. Bright line labels are shown in pink and shadow labels are shown in purple. (a) All of the bright lines connected to all of the shadows. No connections removed. (b) Connections removed that are not between the low and moderate thresholds. (c) Connections added if they are below the relaxed threshold *and* they are connected to a shadow that already has a valid connection that is between the low and moderate thresholds. Building estimates are shown in orange. These estimates are given a label of moderate. (d) Estimates are shown on the SAR image.

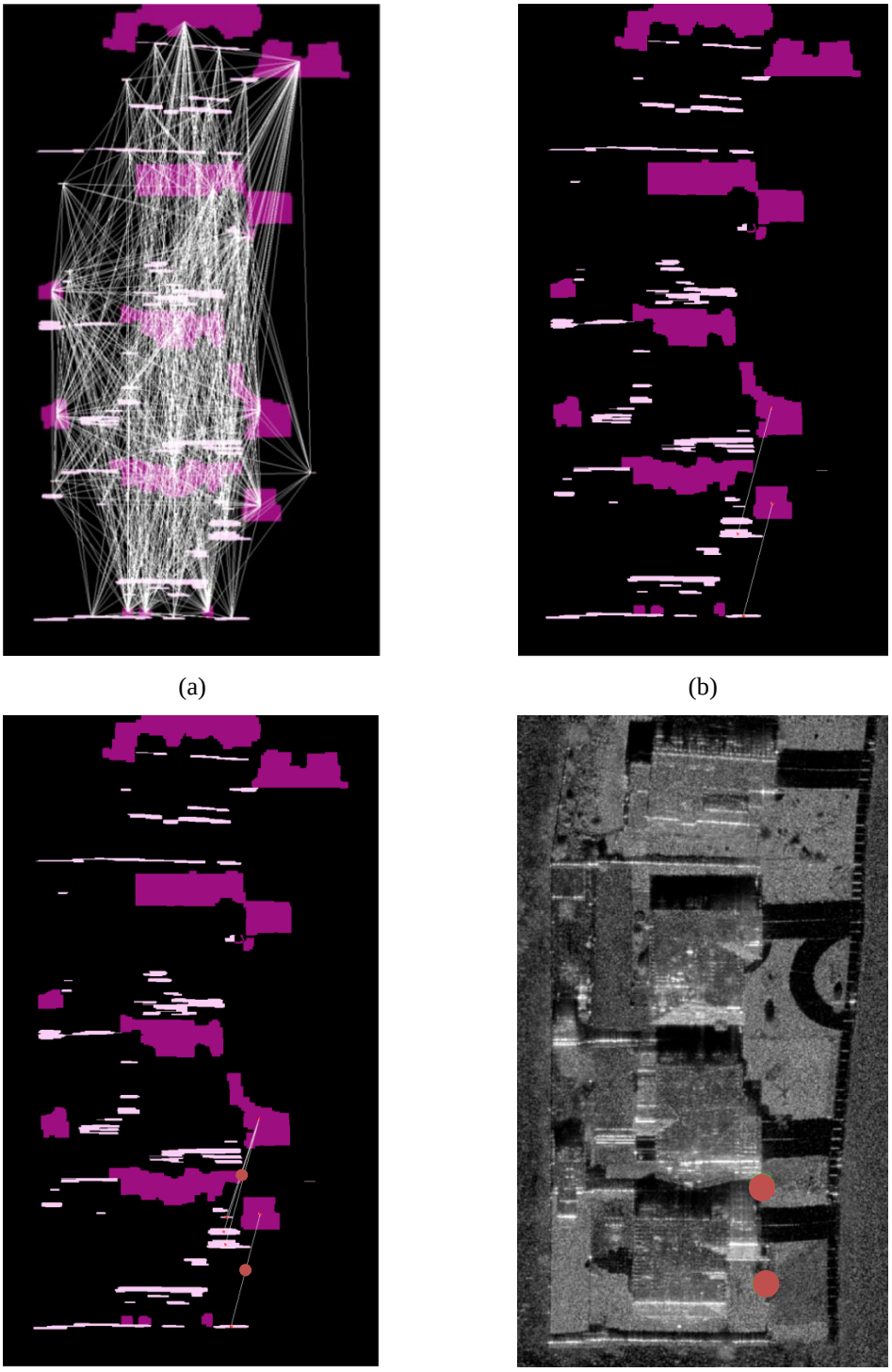

(a) (b)

(c) (d)

Figure 7.6: Weak threshold. Bright line labels are shown in pink and shadow labels are shown in purple. (a) All of the bright lines connected to all of the shadows. No connections removed. (b) Connections removed that are not between the moderate and weak thresholds. (c) Connections added if they are below the relaxed threshold *and* they are connected to a shadow that already has a valid connection that is between the moderate and weak thresholds. Building estimates are shown in red. These estimates are given a label of weak. (d) Estimates are shown on the SAR image.

7.3 Comparison of Results

In order to compare the results, the two techniques must be compared side by side. The results from simple graph grouping are presented in Figure 7.7 a & b. Figure 7.7a shows the accepted connections and the building estimates on the bright line and shadow labels image, and Figure 7.7b shows the building estimates on the SAR image. The green dots used to mark the building estimates do not indicate the label of the estimate (strong, moderate, or weak); all of the estimates created by simple graph grouping are of the same level. The results from weighted graph grouping are presented in Figure 7.7 c & d. Just as for simple graph grouping, Figure 7.7c shows the grouped connections with the building and Figure 7.7d shows the building estimates on the SAR image. Green dots indicate a strong estimate, orange dots indicate a moderate estimate, and red dots indicate a weak estimate.

When the results from the two techniques are compared it is clear that weighted graph grouping is a more robust and powerful technique. If the strong, moderate, and weak estimates (green, orange, and red dots from weighted graph grouping) are all considered valid buildings, then the results from weighted graph grouping are the same as the results obtained from simple graph grouping. However, when only the strong and moderate estimates (green and orange dots from weighted graph grouping) are considered, the false alarms are removed and weighted graph grouping performs better than simple graph grouping. On the other hand, if only the strong estimates (green dots from weighted graph grouping) are considered, the false alarms are removed but also buildings are

missed. This result shows the importance of carefully selecting the thresholds for the different labels if only strong estimates are to be used.

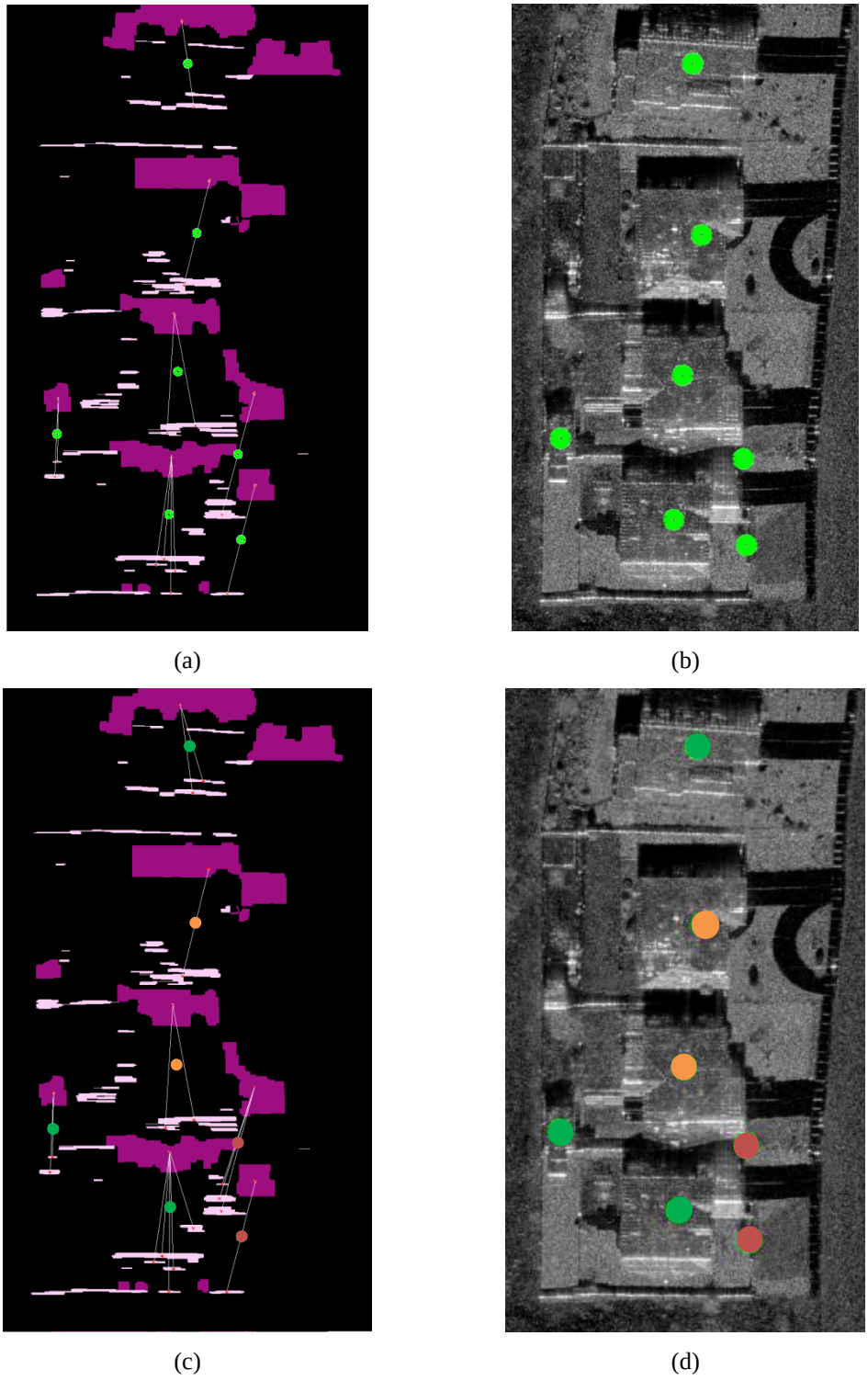

(a) (b)

(c) (d)

Figure 7.7: Bright line labels are shown in pink and shadow labels are shown in purple. (a) Result of simple graph grouping shown on the labeled image. Building estimates are shown as well as the connections which create the estimates. (b) Simple graph grouping estimates shown on the SAR image. (c) Result of weighted graph grouping shown on the labeled image. Building estimates are shown as well as the connections which create the estimates. Green indicates a strong estimate, orange indicates a moderate estimate, and red indicates a weak estimate. (d) Weighted graph grouping estimates shown on the SAR image.

8. Conclusion and Future Work

I have presented two techniques which provide an efficient process to locate buildings in SAR images. They impose minimal restriction or requirements for data collection. The only requirements are that the scene is observed multiple days and the images are co-registered. (The scene needs to be observed multiple days so the bright lines and shadow labels can be generated.) The techniques may not provide a bounding box around the buildings like other techniques, but these techniques are less computationally expensive and do not impose strict requirements for data. By grouping the bright lines and shadows that appear in the image, buildings can be detected. From these groups, the location of the building can be determined. The results show that the techniques are quite valuable and have minimal issues. Although bounding boxes for buildings are not part of the result, the results from both techniques are still very useful because they can provide a starting point to more computationally intensive algorithms which can more accurately and robustly detect the buildings.

In both techniques, false alarms can be present and are in part due to limitations in characterizing and labeling of bright lines and shadows. However, when weighted graph grouping is used, the negative effects from the characterization limitations, building detection false alarms, are minimized because often the estimate is labeled as weak. It is clear that the requirement to accurately label the bright lines and shadows is often a disadvantage of these techniques. Labeling the bright lines and shadows is difficult because there are other objects in the scene that have a backscatter similar to that of the bright lines

and shadows. Cement and water are examples of objects that are similar to shadow, while power lines and other narrow metal objects often appear similar to bright lines. The techniques can be improved by improving characterization techniques such as the enhancement of bright lines and shadows, which are used for grouping the bright lines and shadows.

However, depending on the user expectations for the detector's output, the selection of the best will change. If the user expects a deterministic result and does not want to have to decide how to interpret the label of the estimate, then simple graph grouping would be best. The user would have to accept that all valid connections (even those which barely follow the building assumptions) would be treated as equally likely to be a building. On the other hand, if the user wants the technique to provide a label for the estimate and to work this indication into his or her use of the estimate, then weighted graph grouping would be a better choice. Not only is the detector's output an indicator of which technique should be selected, but the user's knowledge of the scene, confidence in selecting a threshold, resources to create training data, etc., should also factor into the selection of the technique.

If the user has minimal knowledge of the buildings in the scene, then the user should lean toward Weighted Graph Grouping. Weighted graph grouping can easily exploit a generic weighting function and the selection of the thresholds can be tuned by hand. When resources are available to create training data, then it would be beneficial to train the weighting function for Weighted Graph Grouping. (An example of training data would be hand labeled buildings. This would

provide examples of valid connections which provide distance and angle values to train the weighting function.) Simple graph grouping and weighted graph grouping have clear pros and cons, as discussed. Both of these techniques provide an enhancement and improvement to previous techniques, so the selection of the technique is dependent on the application.

To improve and to continue on with this work, it would be of interest to explore more robust and automated techniques for grouping the connection from Weighted Graph Grouping. This would include finding or creating a technique to decide what the best thresholds would be or to cluster the bright lines and shadows using a preexisting clustering algorithm, utilizing the connection weight and the positions of the labels. Another path for further work would be to explore the possibility of training the weighting function or updating it with Bayesian updates.

Appendix. SAR Background

Since the development of radar during World War II, radar has been used for a large variety of applications. These uses span from simple tasks such as object detection and moving target indication, to sophisticated tasks as imaging a large, detailed scenes. Skolnik's *Radar Handbook* discusses several of these applications and the different radar systems [21]. SAR is very useful because it is not hindered by cloud coverage or the need for natural light [9]. As in many systems there are always complications that must be overcome in order to obtain the desired results. SAR provides the increase in cross-range resolution that is required to produce a useful image. SAR allows this increase in resolution without the increase in physical antenna size [20], [21].

SAR allows for the increase of cross-range scene resolution. In order to achieve this, the radar passes over the desired scene. This is often done with an aircraft or satellite. At each position along the path the radar transmits a pulse. The received signal has multiple frequencies corresponding to the Doppler shift of the scene. A Doppler shift is obtained because the scene is stationary and the radar is moving. The radar's velocity must be constant in order to achieve a useable image. By matching the Doppler shifts for each point for all the data, the "synthetic aperture" is achieved [5], [8].

To visualize the improvement in the cross-range resolution one must compare the resolution equations for a real aperture radar (RAR) vs. SAR. For RAR the cross-range resolution δAZ_{RAR}:

$$\delta AZ_{RAR} = \frac{R\lambda}{D} \tag{A.1}$$

where R is the range to the scene, λ is the wavelength of the transmitted pulse, and D is the diameter of the antenna. For SAR (more specifically strip-map SAR) the cross-range resolution δAZ_{SAR}:

$$\delta AZ_{SAR} \approx \frac{D}{2} \tag{A.2}$$

where just as in the RAR equation (equation A.1), D represents the diameter of the antenna. This result follows from the equation A.2 when D is replaced by $2L_{SA}$.

$$\delta AZ_{SAR} \approx \frac{R\lambda}{2L_{SA}} \tag{A.3}$$

where L_{SA} is the path length of the synthetic aperture, and can also be taken to be:

$$\Delta\theta \approx \frac{L_{SA}}{R} \tag{A.4}$$

the synthetic aperture angle. When equation A.4 is substituted into equation A.3 the cross range resolution becomes:

$$\delta AZ_{SAR} \approx \frac{\lambda}{2\Delta\theta} \tag{A.5}$$

For the example of a strip-map SAR, the synthetic aperture angle is:

$$\Delta\theta \approx \frac{\lambda}{D} \tag{A.6}$$

When equation A.6 is substituted in equation A.5, the result shown in equation A.2 is achieved [5], [21].

To take an example from the *Radar Handbook*: For a RAR system with R = 100km, λ = 3cm, and D = 2m, then $\delta AZ \approx$ 1.5km. However, for a SAR system with the same parameters, then $\delta AZ \approx$ 1m [21]. It is clear from the example that the benefit of SAR is that it greatly increases the cross-range resolution.

There are several parameters that must be set correctly in order for the SAR system to function properly. The explanation and guidelines for these parameters are outside of the scope of this appendix but are covered in [5] and [21]. Figure 4.1a (page 14) provides an example of a SAR image.

Since a SAR image is collected at a different wavelength than normal for humans, care must be given when processing the SAR image to not assume it will be similar in every way to an optical image [21]. Skolnik comments on the differences between optical and RF images: "Optical imagery is based on an "angle-angle" principle, whereas SAR imagery is based on a very different "range-cross-range" principle." The result of these different principles is that objects farther from the radar have finer downrange resolution. This is the opposite of the human eye/camera. Another issue that must be considered in SAR is the effect that the topography of the scene has on the resolution at each position. This can result in certain pixels having altered values because there is more area in which the radar collects energy [9].

References

[1] E. Barthelet, G. Mercier, L. Denise, and S. Reynaud, "A new approach for three-dimensional building extraction in high-resolution monoscopic SAR imagery," *9th European Conference on Synthetic Aperture Radar*, Nuremberg, Germany, Apr. 2012, pp. 48-51.

[2] F. Baselice, G. Ferraioli, and D. Reale, "Edge detection using real and imaginary decomposition of SAR data," *IEEE Trans. Geosci. Remote Sens.*, vol. 52, no. 7, pp. 3833-3842, Jul. 2014.

[3] F. Baselice and G. Ferraioli, "Statistical edge detection in urban areas exploiting SAR complex data," *IEEE Geoscience and Remote Sensing Letters*, vol. 9, no. 2, pp. 185-189, Mar. 2012.

[4] Y. Cao, C. Su, and J. Liang, "High resolution SAR building detection with scene context priming," *IEEE 11th International Conference on Signal Processing*, Beijing, China, Oct. 2012, pp. 1791-1794.

[5] J. Curlander and M. Robert, *Synthetic Aperture Radar Systems and Signal Processing*, New York: Wiley, 1991.

[6] G. Ferraioli, "Multichannel InSAR building edge detection," *IEEE Trans. Geosci. Remote Sens.*, vol. 48, no. 3, pp. 1224-1231, Mar. 2010.

[7] A. Ferro, D. Brunner, and L. Bruzzone, "Automatic detection and reconstruction of building radar footprints from single VHR SAR images," *IEEE Trans. Geosci. Remote Sens.*, vol. 51, no. 2, pp. 935-952, Feb. 2013.

[8] T. Freeman (1996, Jan. 26). *What is Imaging Radar* [Online]. Available: http://southport.jpl.nasa.gov/desc/imagingradarv3.html

[9] *InSAR Principles: Guidelines for SAR Interferometry Processing and Interpretation*, TM-19, European Space Agency, Netherlands, Feb. 2007.

[10] M. Jahangir, D. Blacknell, C. P. Moate, and R. D. Hill, "Extracting information from shadows in SAR imagery," *International Conference on Machine Vision*, Islamabad, Pakistan, Dec. 2007, pp. 107-112.

[11] S. M. Kay, "Statistical decision theory I," in *Fundamentals of Statistical Signal Processing: Detection Theory*, vol. 2, Upper Saddle River, NJ: Prentice-Hall, 1998, ch. 3, sec. 3, pp. 63-65.

[12] D. Koller and N. Friedman, "Structure learning in Bayesian Networks," in *Probabilistic Graphical Models: Principles and Techniques*, Cambridge: MIT Press, 2009, ch. 18, sec. 2, pp. 789-790.

[13] A. Kolmogorov, "Sulla determinazione empirica di una legge di distribuzione," *G. Ist. Ital. Attuari*, vol. 4, pp. 83–91, 1933.

[14] P. Lombardo, M. Sciotti, and L. M. Kaplan, "SAR prescreening using both target and shadow information," *Proceedings of the 2001 IEEE Radar*

[15] S. W. MacFaden, J. P. M. O'Neil-Dunne, A. R. Royar, J. W. T. Lu, and A. G. Rundle, "High-resolution tree canopy mapping for New York City using LIDAR and object-based image analysis," *J. Appl. Remote Sens.*, vol. 6, no. 1, Sep. 2012.

[16] M. Moya, "Superpixel segmentations of synthetic aperture radar imagery derived from combinations of multiple data products," *Conference on Data Analysis*, Santa Fe, NM, Mar. 2014, pp. 5-7.*Conference*, Atlanta, GA, 2001, pp. 147-152.

[17] J. P. M. O'Neil-Dunne, S. W. MacFaden, A. R. Royar, and K. C. Pelletier, "An object-based system for LiDAR data fusion and feature extraction," *Geocarto International*, vol. 28, no. 3, pp. 227-242, 2013.

[18] J. P. M. O'Neil-Dunne, K. Pelletier, S. MacFaden, A. Troy, and J. M. Grove, "Object-based high-resolution land-cover mapping," *17th International Conference on Geoinformatics*, Fairfax, VA, Aug. 2009, pp. 1-6.

[19] K. A. Simonson, "Probabilistic fusion of ATR results," *Sandia National Laboratories SAND Report*, Aug. 1998, SAND98-1699.

[20] M. Skolnik, *Introduction to Radar Systems* , 3rd ed., New York: McGraw-Hill, 2001.

[21] M. I. Skolnik, *Radar Handbook*, 3rd ed., New York, McGraw-Hill Professional, 2008.

[22] N. Smirnov, "Table for estimating the goodness of fit of empirical distributions," *Annals of Mathematical Statistics*, vol. 19, pp. 279–281, 1948.

[23] C. Steger, "An unbiased detector of curvilinear structures," *IEEE Trans. Pattern Anal. Mach. Intell.*, vol. 20, no. 2, pp. 113-125, Feb. 1998.

[24] R. Steinbach, M. W. Koch, M. M. Moya, and J. Goold, "Building detection in SAR imagery," *SPIE Defense + Security Radar Sensor Technology XIX*, Baltimore, MD, Apr. 2015.

[25] A. Thiele, E. Cadario, K. Schulz, U. Thonnessen, and U. Soergel, "Building recognition from multi-aspect high-resolution InSAR data in urban areas," *IEEE Trans. Geosci. Remote Sens.*, vol. 45, no. 11, pp. 3583-3593, Nov. 2007.

[26] A. Thiele, E. Cadario, K. Schulz, U. Thonnessen, and U. Soergel, "Building recognition fusing multi-aspect high-resolution interferometric SAR data," *IEEE International Conference on Geoscience and Remote Sensing Symposium*, Denver, CO, 2006, pp. 3626-3629.

[27] Q. Wu, R. Chen, H. Sun, and Y. Cao, "Urban building density detection using high resolution SAR imagery," *2011 Joint Urban Remote Sensing Event*, Munich, Germany, Apr. 2011, pp. 45-48.

[28] L. Zhao, X. Zhou, and G. Kuang, "Building detection from urban SAR image using building characteristics and contextual information," *EURASIP Journal on Advances in Signal Processing*, vol. 2013, no. 1, Dec. 2013.